# New whaitsioids (Therapsida: Therocephalia) from the Teekloof Formation of South Africa and therocephalian diversity during the end-Guadalupian extinction

**Adam K. Huttenlocker** Corresp., [1] , **Roger M. H. Smith** [2, 3]

[1] Department of Integrative Anatomical Sciences, University of Southern California, Los Angeles, California, United States

[2] University of the Witwatersrand, Evolutionary Studies Institute, Johannesburg, South Africa

[3] Iziko South African Museum, Cape Town, South Africa

Corresponding Author: Adam K. Huttenlocker
Email address: huttenlo@usc.edu

Two new species of therocephalian therapsids are described from the upper Permian Teekloof Formation of the Karoo Basin, South Africa. They include two specimens of a whaitsiid, *Microwhaitsia mendrezi* gen. et sp. nov., and a single, small whaitsioid *Ophidostoma tatarinovi* gen. et sp. nov., which preserves a combination of primitive and apomorphic features. A phylogenetic analysis of 56 therapsid taxa and 136 craniodental and postcranial characters places the new taxa within the monophyletic sister group of baurioids—Whaitsioidea—with *Microwhaitsia* as a basal whaitsiid and *Ophidostoma* as an aberrant whaitsioid just outside the hofmeyriid+whaitsiid subclade. The new records support that whaitsioids were diverse during the early-late Permian (Wuchiapingian) and that the dichotomy between whaitsiid-line and baurioid-line eutherocephalians was established early on. The oldest Gondwanan whaitsiid *Microwhaitsia* and additional records from the lower strata of the Teekloof Formation suggest that whaitsioids had diversified by the early Wuchiapingian and no later than *Pristerognathus* Assemblage Zone times. Prior extinction estimates based on species counts are reflected in an analysis of origination/extinction rates, which imply increasing faunal turnover from Guadalupian to Lopingian (late Permian) times. The new records support a growing body of evidence that some key Lopingian synapsid clades originated near or prior to the Guadalupian-Lopingian boundary ca. 260–259 million years ago, but only radiated following the end-Guadalupian extinction of dinocephalians and basal therocephalian predators (long-fuse model). Ongoing collecting in older portions of the Teekloof Formation (e.g., *Pristerognathus* Assemblage Zone) will shed further light on early eutherocephalians during this murky but critical time in their evolutionary diversification.

# New whaitsioids (Therapsida: Therocephalia) from the Teekloof Formation of South Africa and therocephalian diversity during the end-Guadalupian extinction

ADAM K. HUTTENLOCKER[1,*] and ROGER M. H. SMITH[2,3]

[1] Department of Integrative Anatomical Sciences, University of Southern California, Los Angeles, California, U.S.A.;

[2]Evolutionary Studies Institute, University of the Witwatersrand, Johannesburg, South Africa;

[3]Iziko South African Museum, Cape Town, South Africa

*Corresponding author: *ahuttenlocker@gmail.com*

RH: HUTTENLOCKER & SMITH—TEEKLOOF WHAITSIOIDS

**ABSTRACT—**Two new species of therocephalian therapsids are described from the upper Permian Teekloof Formation of the Karoo Basin, South Africa. They include two specimens of a whaitsiid, *Microwhaitsia mendrezi* gen. et sp. nov., and a single, small whaitsioid *Ophidostoma tatarinovi* gen. et sp. nov., which preserves a combination of primitive and apomorphic features. A phylogenetic analysis of 56 therapsid taxa and 136 craniodental and postcranial characters places the new taxa within the monophyletic sister-group of baurioids—Whaitsioidea—with *Microwhaitsia* as a basal whaitsiid and *Ophidostoma* as an aberrant whaitsioid just outside the hofmeyriid+whaitsiid subclade. The new records support that whaitsioids were diverse during the early-late Permian (Wuchiapingian) and that the dichotomy between whaitsiid-line and baurioid-line eutherocephalians was established early on. The oldest Gondwanan whaitsiid *Microwhaitsia* and additional records from the lower strata of the Teekloof Formation suggest that whaitsioids had diversified by the early Wuchiapingian and no later than *Pristerognathus* Assemblage Zone times. Prior extinction estimates based on species counts are reflected in an analysis of origination/extinction rates, which imply increasing faunal turnover from Guadalupian to Lopingian (late Permian) times. The new records support a growing body of evidence that some key Lopingian synapsid clades originated near or prior to the Guadalupian-Lopingian boundary ca. 260–259 million years ago, but only radiated following the end-Guadalupian extinction of dinocephalians and basal therocephalian predators (long-fuse model). Ongoing collecting in older portions of the Teekloof Formation (e.g., *Pristerognathus* Assemblage Zone) will shed further light on early eutherocephalians during this murky but critical time in their evolutionary diversification.

48 INTRODUCTION

49 Therocephalians were a major clade of non-mammalian therapsids whose fossils are best
50 represented in rocks of the middle to late Permian (ca. 272–251.9 million years ago), with a few
51 lineages that survived into the subsequent Triassic Period (Abdala et al., 2008; Huttenlocker et
52 al., 2011). They attained remarkable ecological diversity with wide-ranging body sizes and
53 myriad dental (and, thus, dietary) specializations and other modifications of their feeding
54 apparatus (Kemp, 1972a,b; Huttenlocker, 2014; Huttenlocker and Abdala, 2015; Huttenlocker et
55 al., 2015). Moreover, they are the sister-group to cynodonts—the therapsid group that includes
56 mammals—making them exceptionally important in our understanding of the origins of
57 mammal-like behavior and physiology (Hopson and Barghusen, 1986; Hopson, 1991; van den
58 Heever, 1994; Huttenlocker, 2009). Thus, there has been increasing interest in therocephalian
59 paleobiology in recent years to clarify their evolutionary relationships (Huttenlocker, 2009;
60 Huttenlocker et al., 2011; Kemp, 2012) and to understand their fluctuating diversity patterns
61 within the context of the global biodiversity crises that disrupted terrestrial ecosystems of the late
62 Paleozoic—the end-Guadalupian and Permo-Triassic mass extinctions (Huttenlocker et al., 2011;
63 Huttenlocker, 2014).

64 Despite improvements in our understanding of therocephalian evolution, very little is
65 known about the transition between the middle-to-late Permian, a critical period in the ecological
66 expansion of therocephalians. Early therocephalian fossil localities are globally widespread—
67 particularly in present-day southern Africa and Russia—but their fossils are best known from the
68 middle Permian terrestrial vertebrate assemblages of the Karoo Basin, South Africa (Abdala et
69 al., 2008; Smith et al., 2012). Basal therocephalians of South Africa's middle Permian
70 (Guadalupian) *Tapinocephalus* and *Pristerognathus* assemblage zones (AZ) were large-bodied

apex predators that fell into only a handful of genera and species (Abdala et al., 2008; Abdala et al., 2014). By contrast, the later eutherocephalians that derived from this stock became highly diverse with up to 70 genera (Abdala et al., 2008; Huttenlocker, 2013), and abruptly replaced the earlier, archaic groups in the Karoo Basin by *Tropidostoma* AZ times. These eutherocephalians, along with the gorgonopsians, remained among the most abundant terrestrial predators in early-late Permian terrestrial assemblages in southern Africa (Smith & Botha-Brink, 2011; Smith et al., 2012). Moreover, a major dichotomy between baurioid-line and whaitsiid-line eutherocephalians may have already taken place prior to the early-late Permian *Tropidostoma* AZ, as some museum records of baurioid-line 'ictidosuchids' and whaitsiid-line hofmeyriids were collected from *Pristerognathus* AZ-equivalent rocks of the lower Teekloof Formation (reviewed in Huttenlocker, 2013 and this study).

Among Permian eutherocephalians, whaitsiids have received much taxonomic interest primarily due to the unconventional hypothesis that they may share a relationship with Cynodontia, thus positioning cynodonts within Therocephalia rather than as a close sister-group (Kemp, 1972a; Abdala, 2007; Botha et al., 2007). Although this view has fallen out of favor (van den Heever, 1994; Kemp, 2012; Abdala et al., 2014), little remains known about the diversity of whaitsiid-line therocephalians or the detailed anatomy of their hypothetical common ancestor. The taxonomic history of whaitsioids is complex. Tatarinov (1974) was the first author to include his 'Annatherapsididae' (= Akidnognathidae), 'Moschowhaitsiidae,' and Whaitsiidae within the more inclusive clade 'Whaitsioidea.' However, Mendrez (1974a) separated from Whaitsiidae the akidnognathids and other forms that she did not see fit in either of the two groups, such as the hofmeyriids *Hofmeyria* and *Mirotenthes*—previously regarded as whaitsiids or "forerunners" of whaitsiids by Watson and Romer (1956:70) and other authors (e.g., Attridge,

1956; Brink, 1956). Early cladistic investigations of therapsids also doubted the whaitsiid affinities of akidnognathids and some hofmeyriids (Hopson and Barghusen, 1986; Abdala, 2007), although more recent revisions of therocephalian systematics and phylogeny have supported the traditional view that hofmeyriids likely do share a relationship with whaitsiids (Huttenlocker, 2009; Huttenlocker et al., 2011). Consequently, two major clades of post-akidnognathid eutherocephalians are currently recognized: (1) Baurioidea and (2) a clade of whaitsiids and hofmeyriids to which the term 'whaitsioids' has recently been repurposed (Huttenlocker et al., 2015; Huttenlocker and Sidor, 2016; Maisch, 2017) though it has not been formally defined until now.

**Present Study—** Here, we describe two new therocephalians from the western Karoo Basin that shed light on the poorly known non-mammalian therapsid subclade Whaitsioidea. These whaitsioid records were reported in prior studies (Sidor et al., 2013; Huttenlocker, 2014; Huttenlocker et al., 2015; Huttenlocker and Sidor, 2016), but their anatomy is described and illustrated here for the first time. The specimens were discovered in 1996 and 2011 on two different farms near the border of the Northern and Western Cape provinces, respectively, both from outcrops of the upper Permian Teekloof Formation (Fig. 1). Teekloof-equivalent rocks of the Middleton and lower Balfour formations to the east of the study area have yielded radiometric dates that suggest a relatively continuous sequence of middle to upper Permian rocks in this part of the basin (Rubidge et al., 2013). The combination of constraints on their early-late Permian ages (Wuchiapingian) coupled with their phylogenetic position near the whaitsiid stem makes these new records an important datum for understanding the post-Guadalupian radiation of eutherocephalians and of early non-mammalian therapsid faunas more generally.

## GEOLOGICAL CONTEXT

The Beaufort Group is the most extensively exposed stratigraphic unit of the Karoo foreland basin sequence and consequently the most tetrapod fossils have been recovered from this interval. In the southwestern sub-basin, Beaufort Group sedimentation was initiated by source area tectonism and resulted in the deposition of an approximately 2,700 m thick succession of fluvial channel sandstones and overbank mudrocks (Abrahamskraal and Teekloof formations; Fig. 1) containing rich fossil tetrapod assemblages (i.e., *Eodicynodon, Tapinocephalus, Pristerognathus, Tropidostoma, Cistecephalus*, and *Daptocephalus* AZs of Fig. 1). Sandstone-rich fining-upward packages from 50 to 300 m thick, described as megacycles, occur within the succession. These packages are thought to be related to northeasterly, northwesterly, and east-southeasterly directed fluvial transport systems and subsidence-controlled shifts in the loci of channelization on the alluvial plain (Cole, 1992). The presence of calc-alkaline volcaniclastic detritus and cherts of tuffaceous origin suggests that the provenance rocks in the southwest may have included an active andesitic volcanic chain located on the eastern side of the Andean Cordillera in South America and West Antarctica. Rubidge et al. (2013) dated a series of these tuffs confirming that the Guadalupian-Lopingian boundary occurs close to the top of the Abrahamskraal Formation (Fig.1).

The overlying Wuchiapingian-aged Teekloof Formation in which the new therocephalians were found was deposited by overbank flooding from meandering rivers of variable sinuosity draining an extensive alluvial plain sloping gently towards the northeast in the direction of the receding Ecca shoreline (Turner, 1978). Deposition occurred under semi-arid climatic conditions as evidenced by the presence of desiccation cracks, playa lake evaporite

deposits with desert-rose gypsum aggregates and pedogenic carbonate nodules and lenses (Smith, 1990, 1993). The irregular accretion topography and preferential preservation of upper flow regime plane beds and lower flow regime ripple cross-lamination within channel sand bodies (Smith, 1987) indicates a flood-dominated discharge regime and seasonal inundation of the floodplains resulting in rapid bone burial (Smith, 1993).

The two new therocephalian skulls (SAM-PK-K10984, SAM-PK-K10990) collected from Badshoek (De Hoop 17) are from the same mudrock interval in the middle of the Hoedemaker Member (*Tropidostoma* AZ, +/- 257 Mya). They were found as isolated skulls and were encrusted with a 2 mm-thick layer of pedogenically-precipitated micrite. Associated dicynodont taxa collected in the same strata include *Tropidostoma, Emydops, Pristerodon* and *Diictodon*, as well as a small gorgonopsian (see Table 1).

The Good Luck (Matjiesfontein 412) specimens (SAM-PK-K8516, SAM-PK-K8631) were collected from massive gray siltstone beds in the upper Oukloof Member (upper *Cistecephalus* AZ, +/- 255 Mya) along with several skulls and partial skeletons of *Cistecephalus*, *Oudenodon*, *Diictodon, Procynosuchus* and *Pareiasaurus* (see Table 1).

## MATERIAL AND METHODS

The electronic version of this article in Portable Document Format (PDF) will represent a published work according to the International Commission on Zoological Nomenclature (ICZN), and hence the new names contained in the electronic version are effectively published under that Code from the electronic edition alone. This published work and the nomenclatural acts it contains have been registered in ZooBank, the online registration system for the ICZN. The

ZooBank LSIDs (Life Science Identifiers) can be resolved and the associated information viewed through any standard web browser by appending the LSID to the prefix http://zoobank.org/. The LSID for this publication is: urn:lsid:zoobank.org:pub:4D798F6D-74BC-4FE8-BA46-79DAA314FE09. The online version of this work is archived and available from the following digital repositories: PeerJ, PubMed Central and CLOCKSS.

## SYSTEMATIC PALEONTOLOGY

### THERAPSIDA Broom, 1905

### THEROCEPHALIA Broom, 1903

### EUTHEROCEPHALIA Hopson and Barghusen, 1986

### WHAITSIOIDEA Tatarinov, 1974

**Composition**—*Theriognathus microps* Owen, 1876; *Ictidostoma hemburyi* (Broom, 1911); *Hofmeyria atavus* Broom, 1935; *Ictidochampsa platyceps* Broom, 1948; *Mirotenthes digitipes* Attridge, 1956; *Moschowhaitsia vjuschkovi* Tatarinov, 1963; *Viatkosuchus sumini* Tatarinov, 1995; *Microwhaitsia mendrezi* gen. et sp. nov.; *Ophidostoma tatarinovi* gen. et sp. nov.

**Definition**—The most inclusive clade that contains *Theriognathus microps* and *Ictidostoma hemburyi*, but not *Ictidosuchus primaevus* and *Bauria cynops* [stem-based].

**Revised diagnosis**—Small- to large-bodied therocephalians having a wide suborbital bar forming well-frontated orbits; ventromedially infolded maxilla with medially positioned tooth row so that much of the maxillary facial lamina is visible in ventral view; anterior border of orbit

186 is located on anterior half of skull (conv. in cynodonts, *Lycosuchus*, some akidnognathids, and
187 derived bauriamorphs); epipterygoid anteroposteriorly expanded; epipterygoid processus
188 ascendens anterior edge orientation in lateral view is strongly anterodorsal (rather than
189 posterodorsal or vertical) producing an anvil-shape; dentary tall and boomerang-shaped; and
190 dentary ramus lateral groove weak (*Ophidostoma*) or absent (all others).
191
192 WHAITSIIDAE Haughton, 1918
193
194 **Composition**—*Theriognathus microps* Owen, 1876; *Ictidochampsa platyceps* Broom,
195 1948; *Moschowhaitsia vjuschkovi* Tatarinov, 1963; *Viatkosuchus sumini* Tatarinov, 1995;
196 *Microwhaitsia mendrezi* gen. et sp. nov.
197 **Definition**— The most inclusive clade that contains *Theriognathus microps* and
198 *Viatkosuchus sumini*, but not *Ictidostoma hemburyi* and *Hofmeyria atavus* [stem-based].
199 **Revised diagnosis**—Medium-to-large eutherocephalians with median frontonasal crest
200 (also in *Chthonosaurus* and akidnognathids); suborbital vacuities reduced in size or absent;
201 prefrontal and postorbital nearly contact, limiting contribution of frontal to dorsal border of orbit;
202 epipterygoid extremely expanded anteroposteriorly (more so than hofmeyriids); epipterygoid
203 posterior apophysis forms specialized "trigeminal notch"; pterygoid boss teeth usually absent
204 (though present in *Viatkosuchus*).
205
206 *MICROWHAITSIA MENDREZI* gen. et sp. nov.
207 (Figs. 2-6)
208

**Etymology—***Micro* (Greek, 'small'); *whaitsia* (refers to whaitsiid affinities). Species epithet honors Christiane Mendrez-Carroll for her substantial contributions to the morphology and systematics of therocephalians.

**Holotype—**Iziko South African Museum (SAM) PK-K10990, partial skull with dentaries preserved in occlusion, missing most of the braincase, occiput, and postdentary bones (Figs. 2–4).

**Referred specimen—**SAM-PK-K10984, weathered snout preserving most of the left antorbital region, palate, and maxillary canine and postcanine alveoli (Figs. 5–6).

**Locality and horizon—**Both specimens were collected by RMHS in 2011 from Badshoek farm (De Hoop 117) near Beaufort West District, Western Cape Province, Republic of South Africa; upper *Tropidostoma* Assemblage Zone (Wuchiapingian stage), upper Permian Teekloof Formation (Hoedemaker member). Detailed locality information is available at Iziko South African Museum, Cape Town.

**Diagnosis—**Small-to-medium sized therocephalian with broad, robust skull; nasals strongly waisted at mid-length in dorsal view; thickened, pachyostotic frontal bone; thickened suborbital bar (nearly as deep as the orbit's dorsoventral height); upper dental formula I5:pC1:C1:PC5; lower dental formula i4:c1:pc5.

## General Description

In general, the two specimens of *Microwhaitsia* show a robust snout, cheek, and dentition, and are similar to each other in overall size (estimated skull lengths ~180 mm). The skull roofs are strongly sutured and craniofacial bones fairly thick for their small size. The holotypic skull--SAM-PK-K10990--is nearly complete with dentition and both lower dentaries

intact in occlusion, but it is missing much of the occiput and intertemporal region, as well as the postdentary bones. The referred specimen--SAM-PK-K10984--is a weathered snout and left antorbital region, missing the premaxilla, and most of the right side of the skull. The dentition is also missing from the referred specimen. In both specimens, cranial sutures are easily distinguished and tend to be noticeably sinuous and interdigitating, with few straight sutures except along the midline. The braincase and occiput are not preserved in either specimen.

**Skull Roof**

The premaxilla is a three-part element consisting of maxillary, vomerine, and dorsal (internarial) processes. The maxillary portion bears a short interdigitating suture with the maxilla that borders a small nervous foramen and, more dorsally, the septomaxillary foramen. Dorsally, the internarial process forms the medial septum of the naris and is fairly short, not reaching posteriorly beyond the level of the septomaxilla. The holotype preserves five premaxillary (incisor) alveoli. The septomaxilla is a rather large, solid element, but it is not well exposed outside of the naris. There is a modest dorsal process within the naris. The ventral footplate shares little overlap with the premaxilla externally, and the posterior facial process is fairly short dorsal and medial to the septomaxillary foramen.

The maxilla is the dominant element of the rostrum, having an exceptionally high facial lamina. The facial lamina is so high and broad and that very little of the nasal can be seen in lateral view (Figs. 2, 3). It is highest anteriorly and, when viewed laterally, rapidly tapers just behind the anterior border of the orbit ventral to the jugal. The lateral surface of the rostrum is coarsely pitted by many nervous foramina in front of the antorbital depression. In ventral (palatal) view, the maxilla borders a fossa for the lower canine and expands behind this area forming a crista choanalis (Fig. 4). The crista is sufficiently expanded that it just contacts the

255 vomer dorsally (Fig. 4B), separating the anterior (canine fossa) and posterior portions of the
256 choana. However, there is no true maxillovomerine bridge as the connection is not sutural
257 (unlike *Theriognathus* and *Moschowhaitsia* where the two elements are sutured). Attachment
258 sites for maxilloturbinates on the medial side of the facial lamina could not be discerned.

259 The nasal is relatively long and narrow despite the broad, round profile of the snout. This
260 is in part influenced by the large size of the maxilla facial laminae, which give the nasals a
261 waisted appearance along their mid-length in dorsal view.

262 The lacrimal is a short, square element on the anterolateral margin of the orbit. It is much
263 abbreviated due to the tall, broad facial lamina of the maxilla. Dorsally, it is bordered by the
264 anterior tongue of the prefrontal, which contacts the maxilla and, thus, bars the lacrimal from
265 contacting the nasal, as in most other therocephalians (except lycideopids). Just anterior to the
266 orbit, near the contacts with the jugal and maxilla, there is a marked antorbital fossa which bears
267 the lacrimal foramina (as in the therocephalian *Hofmeyria* and, convergently, burnetiamorph
268 therapsids). One large foramen occupies a position on the anterior rim of the orbit, whereas the
269 other smaller foramen is situated more ventrolaterally near the jugal-maxilla suture. The details
270 of the nasolacrimal canal and its communication with the internal (medial) face of the maxilla
271 could not be determined at present.

272 The prefrontal forms the anteromedial border of the orbit. It contacts the lacrimal
273 ventrolaterally and the maxilla and nasal anteriorly. The posterior process does not contact the
274 postorbital over the orbit, so that a small portion of the frontal contributes to the margin of the
275 orbit. The prefrontal and postorbital nearly meet inside the orbit as in *Theriognathus* (Fig. 2C).

276 The frontal is very thick and pachyostotic (~13 mm thick at midorbit level). In dorsal
277 view, it is roughly diamond-shaped with stout lateral processes narrowly contacting the orbital

margin. The element's anterior extent just reaches the level of the anterior margin of the orbit where it strongly interdigitates with the nasal. There is a prominent median frontonasal crest on the midline as in other whaitsiids. The midline suture is comparatively straight except at the midorbit level where it becomes noticeably jagged.

The postorbital bounds the posteromedial margin of the orbit. The postorbital bar is robust and strongly sutures to the jugal. Most of the bar is formed by the broad postorbital process of the jugal. As in *Theriognathus* and other whaitsiids, the jugal is a substantial element, promoting the robust appearance of the skull despite its small size. However, the total depth of the suborbital bar is more so than in other whaitsiid genera, being 40-50% the height of the skull (nearly as tall as the orbit itself) (Figs. 2C, 3C). By contrast, hofmeyriids have comparatively thin suborbital bars (e.g., *Hofmeyria*, *Mirotenthes*).

**Braincase and Occiput**

Most of the braincase and occiput are missing from the specimens. However, the bisected referred specimen clearly shows portions of the sphenethmoid preserved in place. The sphenethmoid complex has been described in a few therocephalians, including *Ictidosuchoides* (Crompton, 1955), *Microgomphodon* (Abdala et al., 2014), *Tetracynodon* (Sigurdsen et al., 2012), and *Theriognathus* (Kemp, 1972; Huttenlocker and Abdala, 2015). The anterodorsal portion of the sphenethmoid complex, the orbitosphenoid, resides just dorsal and posterior to the vomer, forming a broad but thin ascending lamina that would have made up the anteromedial wall of the orbit. As in *Tetracynodon*, there is a broadly convex notch along its posterior margin that may have accommodated the optic nerve (Sigurdsen et al., 2012: fig.2). Its dorsal most extent nearly contacts the ventral surface of the frontal, but is separated by a small fissure.

**Palate, Splanchnocranium, and Suspensorium**

The vomer is best viewed in palatal aspect in the holotype. It has a long interchoanal process that widens anteriorly as in other therocephalians and is widest at its anterior contact with the premaxilla. Although the crista choanalis just contacts the vomer anterodorsally, creating the appearance of a strongly vaulted palate, there is no true maxillovomerine bridge. There is a modest median crest that runs longitudinally along the vomer's ventral margin, and a suture that separates the vomer into right and left halves spans the entire posterior region and much of the length of the interchoanal process (as in basal therocephalians and some hofmeyriid specimens).

The crista choanalis is short and smoothly rounded, rolling onto the palatine and terminating just anterior to the suborbital vacuity. As in other whaitsiids, there are at least two prominent ridges formed in this region: one that is confluent with the vomer-palatine suture emarginating the choana and a second that is more laterally positioned and confluent with the palatine-maxilla suture and alveolar margin (Figs. 5B, 6B). The maxilla-palatine foramen is positioned somewhat posteriorly, just medial to the first and second postcanines. The ectopterygoid is preserved on the left side of the skull in the referred specimen. It formed a narrow strut bracing between the palatine, maxilla, and jugal along the anterolateral margin of the suborbital vacuity. It is pierced ventrally by a small foramen. Little of the pterygoid could be discerned in either specimen. Likewise, the epipterygoid and the suspensorium (including the quadrate-quadratojugal complex) are not preserved in either specimen.

**Mandible**

Portions of the left and right lower jaws are preserved in the holotypic specimen, including the left and right dentaries and splenials, right coronoid, right prearticular, and right surangular. The dentary is a robust element with a thick mentum that was only loosely sutured at

the symphysis. The overall shape is strongly bowed as in other whaitsioids. The lateral surface of the ramus is smooth, bearing no dentary groove or trough. The anterior surface of the mentum is pitted with fine vascular foramina. The coronoid process is very tall, terminating in the upper half of the orbit, and its terminal margin is slightly rounded. On the medial surface of the dentary, a long, flat splenial can be seen running anteriorly and meeting on the left and right sides just behind the dentary symphysis. Just posterior and dorsal to the splenial on the right side, a single coronoid and anterior portions of the prearticular are preserved, bounding the anterior and lower parts of the mandibular fenestra. The anterior half of the surangular is preserved on the medial surface of the dentary coronoid process and forms the upper border of the mandibular fenestra. The majority of the postdentary region is not preserved.

**Dentition**

The dentition is best preserved in the holotypic specimen, although maxillary alveoli are also present in the referred specimen. The holotype preserves five upper incisors, one upper precanine, one upper canine (a second root of a previously functional canine is also preserved on the left side of the skull immediately behind the newly functional canine), and five upper postcanines. The dentary preserves four lower incisors, a single lower canine, and five lower postcanines. As in most whaitsioids and early eutherocephalians in general, longitudinal fluting of the enamel was likely present on the incisors based on the fifth left upper incisor, which is the best preserved. However, most of the dentition is highly abraded, making the enamel texture difficult to examine. In general, the incisor crowns are subcircular in cross-section and lack serrations or mesio-distal carinae. The upper canine is fairly large, subcircular in cross-section, and also lacks serrations or carinae. Following a short diastema, the postcanines are preserved as simple, conical crowns that are subcircular in cross-section. These also lack any serrations or

mesio-distal carinae. The surface enamel of the postcanines is too poorly preserved to discern any postcanine fluting.

WHAITSIOIDEA incertae sedis

*OPHIDOSTOMA TATARINOVI* gen. et sp. nov.

(Figs. 7-8)

**Etymology—**Tatarinov's 'snake mouth.' *Ophido-* (Greek, 'snake' or 'serpent'); *stoma* (Greek, 'mouth'). Genus name refers to the wide gape permitted by the loose mandibular symphysis and streptostylic jaw of whaitsioid therocephalians. Species epithet honors Leonid Tatarinov for his contributions to whaitsioid systematics and therocephalian functional anatomy.

**Holotype—**SAM-PK-K8516, weathered skull and articulated mandible missing portions of palate and braincase (Figs. 7–8).

**Locality and Horizon—**The specimen was collected by RMHS in 1996 on **'**Good Luck' farm (Matjiesfontein 412) near Fraserburg District, Northern Cape Province, Republic of South Africa; upper *Cistecephalus* Assemblage Zone (Wuchiapingian stage), upper Permian Teekloof Formation (Oukloof member). Detailed locality information is available at Iziko South African Museum, Cape Town.

**Diagnosis—**Small therocephalian with short, broad skull (greatest skull breadth at occiput approximately equal to basal skull length); frontal length-to-width ratio approximately 1.0; pineal opening situated on raised boss; pterygoid boss teeth present; upper dental formula: I?:C1:PC6. Plesiomorphic in the retention of longitudinal striae/fluting on upper postcanines (primitive for eutherocephalians).

370

371 **General Description**

372 The specimen consists of a small, poorly preserved skull and mandible (skull length from
373 occipital condyle to tip of snout ~60-65 mm), with the right side of the skull slightly crushed and
374 the lower jaw laterally displaced. Its most recognizable features are the stout rostrum and the
375 broad zygoma, producing a skull that is as wide as it is long.

376 The specimen was prepared using a pneumatic scribe so that most of the outer surface of
377 the skull roof and mandible was exposed, and the ventral surface prepared to the palate. The
378 skull was then scanned using high-resolution X-ray computed tomography (HRXCT) at the
379 University of Utah Core Imaging Facility to reveal aspects of the palate, cranial sinuses, and
380 braincase. It was scanned using an Inveon µ-CT scanner with scanner settings: 100 kV and 60
381 µA with a voxel size of 90 µm. Stacks were volumized and studied in OsiriX (Rosset et al.,
382 2004). Unfortunately, the HRXCT data revealed that much of the palate and basicranium was
383 'blown-out' prior to fossilization, leaving only the skull roof, peripheral portions of the braincase
384 and basicranium, and mandible.

385 The specimen has suffered from slight pre-burial distortion, including flaring of the right
386 cheek and loss of the right zygoma, allowing ventrolateral displacement of the dentary ramus,
387 although connection to the left dentary at the symphysis was maintained (Figs. 7D, 8D). The
388 squamosal is also displaced slightly anteriorly within the temporal fossa on both sides. This
389 distortion has led the authors to consider the possibility that the striking breadth of the skull
390 relative to its short length was a result of postmortem crushing or other deformation. However,
391 these proportions likely did not result from preservational artifact because large portions of the

skull roof are preserved in articulation and some *in situ* cranial calvariae are clearly broad with their widths being subequal to or slightly greater than their lengths (e.g., frontal).

**Skull Roof**

The maxilla is a very tall element with a broad facial lamina. The canine was deeply rooted, although it is mostly weathered and missing the entire crown. As in other whaitsioids, the facial lamina of the maxilla gently rolls onto the ventral (palatal) surface to meet the abbreviated alveolar margin (Figs. 7B, 8B). There are six closely packed postcanines situated along the alveolar margin on the right side of the skull. In palatal view, the choana can be seen to have been short and the crista choanalis also fairly short and rounded (rather than sharp medially). The medial surface of the facial lamina is smooth and shows no evidence for attachment of maxillary turbinates as in most other therocephalians (Huttenlocker et al., 2011; Sigurdsen et al., 2012; but see Hillenius, 1994). Internally, there is a large, cavern-like anterior maxillary sinus (sensu Sigurdsen, 2006) as in other therocephalians that have been serially sectioned or CT scanned (Sigurdsen et al., 2012). The sinus opens anteriorly onto the medial surface of the maxilla. A posterior duct parallels the tooth row, leading into a smaller sinus (the posterior maxillary sinus; sensu Sigurdsen, 2006) that opens posteriorly into a shallow fossa on the medial surface of the maxilla just behind the tooth row.

The nasals are imperfectly preserved in SAM-PK-K8516, with most of the left side weathered away and the right badly fractured. Surface features and nasoturbinal ridges could not be discerned due to this damage. In life, the nasals would have been fairly short and broad as in the other skull roof elements.

The lacrimal is a square element that forms part of the anterior wall of the orbit and extends internally onto the palate. Two small nasolacrimal foramina located on the anterior

margin of the orbit open into the nasolacrimal canal. The canal forms a narrow caliber duct that opens onto the medial surface of the facial lamina of the maxilla near the maxilla-lacrimal suture.

The prefrontal is a tall and broad element that forms most of the anteromedial margin of the orbit. It is fairly fractured on the right side of the skull and slightly weathered on the left so that its precise suture contacts are difficult to determine. However, given its breadth and the high facial lamina of the maxilla, it is likely that it contacted the maxilla anteriorly so that a nasolacrimal contact was not permissible as in most therocephalians.

The frontal forms a broad diamond that is as wide as it is long, a rare feature in a therocephalian. The interorbital breadth is therefore relatively wider than in other therocephalians. The dorsal surface is flat and smooth so that there is no median frontonasal crest. The frontal contributes strongly to the dorsomedial wall of the orbit, widely separating the prefrontal and postorbital. This contrasts with the condition in other whaitsioids where the latter elements contact in the upper wall of the orbit (hofmeyriids) or nearly contact along its dorsal margin (whaitsiids).

The postorbital is a lunate element forming most of the posterior border of the orbit. Its jugal process is long and robust, although its connection to the jugal is not preserved due to damage to the zygoma on both sides of the skull. More posteriorly, the postorbital broadly overlaps the parietal extending beyond the level of the pineal foramen.

The jugal is incompletely preserved, forming only a portion of the ventrolateral margin of the orbit and missing the postorbital and zygomatic processes. Based on the preserved portions, the suborbital bar was very slender as in *Hofmeyria* and *Mirotenthes*. The squamosal is disarticulated on both sides of the skull, being displaced anteromedially into the temporal fossa. It is tall and thin with a broadly concave anterior face that, when articulated, overlapped the

supraoccipital, interparietal, and parietal. The sutural overlap with the parietal was extensive as in the postorbital.

The parietal is a tall element forming the dorsolateral walls of the braincase, which are vertical and parallel-sided as in other eutheriodonts. The parietal (sagittal) crest is short behind the pineal foramen. Internally, the enclosure forming the pineal canal is deep and the external opening large and situated on an elevated parietal boss. The interparietal could not be discerned with certainty due to crushing in this region and anterior displacement of the supraoccipital.

**Braincase and Occiput**

Very little of the braincase and occiput are preserved in SAM-PK-K8516. The sphenethmoid complex could not be observed in the prepared specimen or in the CT scans. Small portions of the wedge-shaped supraoccipital are preserved on the left and right sides of the skull in close association with the parietal. Ventral to this, a tiny portion of the right exoccipital is preserved in contact with the basioccipital where the two would have bounded the foramen magnum. There is a strong basicranial girder formed between the ventromedian keel of the parabasisphenoid and the paired parasagittal processes of the pterygoid. The basal tubera are of moderate size (approximately 25% the width of the skull). The prootics and opisthotics are too poorly preserved to describe in detail.

**Palate, Splanchnocranium, and Suspensorium**

Much of the palate is unpreserved so that the relationships between the vomer, palatines and ectopterygoids cannot be described in detail. The maxillae bear a modest crista choanalis that border a fairly short choana. The crista is low and rounded, rather than sharp and distinct. Although the vomer is not preserved, a maxillovomerine bridge was likely to have been absent based on the lack of obvious medial (palatal) processes of the maxilla near the level of the canine

461 or posterior to it. Portions of the pterygoid are preserved more posteriorly, showing well-
462 developed transverse flanges that formed the posterior border of the suborbital vacuity. The
463 flanges sweep medially and posteriorly where they formed paired parasagittal ridges bounding a
464 wide interpterygoid vacuity. Pterygoid boss teeth are present, with three small, longitudinally
465 arranged denticles present on the right and a large tooth preserved centrally on the left boss. The
466 quadrate processes and the dorsally adjoining epipterygoid are not preserved. A massive element
467 that rests within the quadrate recess of the squamosal on the left side of the skull is interpreted
468 tentatively as the quadrate-quadratojugal complex.

469 **Mandible**

470 The mandible is preserved on the left and right sides of the skull. The left mandible is
471 largely in place and held in occlusion, whereas the right is slightly ventrolaterally displaced and
472 disarticulated. The dentary is long and strongly bowed, with the distinctive boomerang-shape
473 that is common amongst whaitsioids. The coronoid process is broken on the left side, but is
474 preserved on the right where it can be seen as an extremely tall element. This tall process would
475 have terminated in the upper half of the temporal fenestra as in *Hofmeyria* and *Mirotenthes*. Its
476 terminal margin is somewhat rounded. Along the ramus, there is a very modest lateral dentary
477 groove (or trough), unlike in other whaitsioids that lack this feature entirely. Internally, there is a
478 large nervous canal that runs the length of the dentary, dorsal to the Meckelian groove, and feeds
479 the alveoli. Medially, portions of the prearticular are preserved in contact with the Meckelian
480 groove in the left side. The dentary, prearticular, and angular border a fairly large mandibular
481 fenestra as in other eutherocephalians. The angular bears a broad but thin reflected lamina with
482 radiating ridges and a dorsal notch. The surangular borders the reflected lamina dorsomedially.
483 The presence of an articular in the specimen could not be confirmed.

**Dentition**

Due to damage to the premaxilla, the upper incisors are not preserved in the specimen. The upper canines are large and deeply rooted, although their crowns have also weathered away almost completely. Six postcanines are present in the right maxilla, although the roots of only three are preserved on the left. The crowns are short, conical with circular cross-sections and lacking carinae, and bear fine longitudinal striae on their external surface as in some basal akidnognathids (i.e., *Akidnognathus*) and baurioids (i.e., *Ictidosuchus*). Just anterior to the position of the second postcanine, a replacement tooth can be seen emerging from the maxilla on the right side.

Most of the lower incisors are missing, although a single pair of incisors (presumably in the fourth position) is preserved on both the left and right dentary, each pressed against the mesial surfaces of the lower canines. Their surface texture is abraded such that the presence of enamel striae (as in the postcanines) cannot be confirmed. The tooth row is very short with most of the teeth (including the postcanines) restricted to the anterior third of the dentary. There are at least four (and likely more) lower postcanines packed tightly together behind the lower canine. The anteriormost postcanine in the right dentary preserves enamel striae.

## RESULTS & DISCUSSION

**Phylogenetic Position of New Whaitsioids**

Whereas early cladistic investigations regarded hofmeyriids as relatively basal eutherocephalians (Hopson and Barghusen, 1986; Abdala, 2007), more recent studies have supported that they are most closely related to whaitsiids, such as *Theriognathus* (Huttenlocker

and Abdala, 2015). Prior to the present study, the holotypic specimens of *Microwhaitsia* and *Ophidostoma* were incorporated into a preliminary phylogenetic analysis and were referenced only by their voucher numbers (Huttenlocker, 2014; Huttenlocker et al., 2015; Huttenlocker and Sidor, 2016). We assessed the phylogenetic positions of *Microwhaitsia* and *Ophidostoma* using a matrix of 136 craniodental and postcranial characters from 56 therapsid taxa (including two outgroups *Biarmosuchus* and *Titanophoneus*, plus 54 neotherapsid ingroup taxa) (see Supplementary Appendices S1 and S2). The data were analyzed in PAUP*4.0b10 (Swofford, 1999) and MrBayes v. 3.2.6 (Ronquist et al., 2009). A heuristic search was performed in PAUP using maximum parsimony with a random addition sequence with 100 replicates and the tree-bisection-reconnection (TBR) branch-swapping algorithm. Characters were not ordered and all given equal weight. Multistate characters were interpreted as uncertainty. The Bayesian analysis was performed using the standard Mk model for morphological evolution (Lewis, 2001) with variable character rates. We ran the analysis for one million generations (with the first 25% removed as burn-in) and sampled the posterior distribution every 100 generations.

Parsimony analysis recovered 1160 equally most parsimonious trees (MPTs) having a length of 381 steps (consistency index (CI) = 0.438; retention index = 0.789; rescaled CI = 0.346). The analysis found Hofmeyriidae, Whaitsiidae, and Baurioidea to represent monophyletic clades nested within Eutherocephalia. The high number of MPTs differed only in their volatile arrangements of basal scylacosaurid therocephalians, basal (ictidosuchid-grade) baurioids, and Triassic bauriids. Though the major (deep) branches of eutherocephalians are relatively stable, there were notable differences between parsimony and Bayesian-based approaches. In particular, the interrelationships of basal therocephalians are poorly resolved in the Bayesian topology, which fails to support the monophyly of Scylacosauridae. Moreover, the

Bayesian topology yields a major eutherocephalian polytomy between Perplexisauridae, Chthonosauridae, Akidnognathidae, and the Whaitsioidea+Baurioidea clade. It also recovers the baurioid family Lycideopidae as the monophyletic sister-group to Bauriamorpha, while the parsimony trees recover Lycideopidae as a paraphyletic assemblage that includes Bauriamorpha as a subgroup. To account for these uncertainties, we present a conservative topology in Figure 9 that illustrates the conflicting parsimony and Bayesian arrangements as polytomies.

All of the MPTs retrieved a monophyletic Whaitsiidae composed of the Permian eutherocephalians *Ictidochampsa* (Broom, 1948), *Viatkosuchus* (Tatarinov, 1995), *Moschowhaitsia* (Tatarinov, 1963), and *Theriognathus* (Owen, 1876). *Microwhaitsia* is found to be nested within whaitsiids as the sister-taxon to *Viatkosuchus* + (*Moschowhaitsia* + *Theriognathus*). Among whaitsioids, characters shared between *Microwhaitsia* and other whaitsiids include: median frontonasal crest present; suborbital bar robust, deepened; postorbital bar moderately well built (extremely slender in hofmeyriids and baurioids); prefrontal and postorbital nearly contact on dorsomedial wall of orbit; upper postcanines reduced to five or fewer. Based on the character evidence, *Viatkosuchus* and *Microwhaitsia* would together represent the geologically oldest occurrences of whaitsiids in Laurasia and Gondwana, respectively (discussed further below).

*Ophidostoma* is found to be nested within Whaitsioidea, but the specimen does not demonstrate clear features that unite it with any given whaitsioid subgroup. Based on gross similarities to hofmeyriids, Huttenlocker et al. (2015) labeled *Ophidostoma* as '*Cistecephalus* AZ hofmeyriid' (Huttenlocker et al., 2015:fig. 6). However, the present analysis shows that *Ophidostoma* falls outside the clade that includes the closest common ancestor of Hofmeyriidae+Whaitsiidae, indicating that it is an aberrant whaitsioid and that its hofmeyriid-

like gestalt represented plesiomorphies shared by all whaitsioids.

**Whaitsioidea-Baurioidea dichotomy—**The present phylogenetic hypothesis further implies a major dichotomy between two non-akidnognathid eutherocephalian radiations during the Permian: Whaitsioidea and Baurioidea. In general, the whaitsioids were characterized by small and large-bodied species (skull lengths ranging ~6–35 cm) with a broad cranium having greater area for the jaw adductor musculature, a robust, boomerang-shaped mandible, and a tendency toward reduction of the postcanine teeth, whereas baurioids typically consisted of small to mid-sized species (skull lengths ranging ~5–20 cm) with a low, slender rostrum and numerous postcanines. A close relationship between whaitsioids and baurioids was originally demonstrated by Huttenlocker (2009), who suggested that their common ancestry could be traced to no later than the middle-to-late Permian transition during *Pristerognathus* AZ times.

Unlike Ivakhnenko's (2011) usage of 'Whaitsioidea' which included lycosuchids and akidnognathids as subgroups—thus, making the name equivalent to Therocephalia—we define Whaitsioidea explicitly as the most inclusive clade that contains *Theriognathus microps* and *Ictidostoma hemburyi*, but not *Ictidosuchus primaevus* and *Bauria cynops* [stem-based]. As such, the group includes representative hofmeyriid and whaitsiid taxa (e.g., *Hofmeyria*, *Theriognathus*), but excludes akidnognathids and baurioids. Permian whaitsioids share a number of craniodental synapomorphies that distinguish them from the latter two groups, including: a wide suborbital bar forming well-frontated (i.e., forward-facing) orbits; ventromedially infolded maxilla facial lamina with concave alveolar margin (rather than convex as in some akidnognathids, or straight as in all others); anterior border of orbit located on anterior half of skull; anvil-shaped epipterygoid processus ascendens with anterior tilt (see below); broad contact between processus ascendens and parietal; dentary strongly bowed or boomerang-shaped;

576 dentary ramus lateral groove/furrow weak (*Ophidostoma*) to absent. Some of these features have
577 been discussed elsewhere (Huttenlocker, 2009; Huttenlocker et al., 2011). Additional features of
578 the braincase shared by whaitsioids may be elucidated with further computed tomographic
579 research. The external morphology of the whaitsioid braincase also exhibits an anteriorly tilted
580 epipterygoid with an anterodorsally oriented leading edge of the processus ascendens (Figure 10)
581 as demonstrated by a specimen of the hofmeyriid *Mirotenthes* (SAM-PK- K11188) recovered
582 from coeval *Cistecephalus* AZ deposits at 'Good Luck' in association with *Ophidostoma*. This
583 contrasts with the more upright or posteriorly leaning epipterygoid of baurioids (e.g., Sigurdsen
584 et al., 2012:fig. 2) and other therocephalians (e.g., Huttenlocker et al., 2011:fig. 4). The
585 orientation of the processus ascendens has been incorporated as new character 136 in the present
586 phylogenetic analysis.

587 **Evolution of early eutherocephalian dental morphology and surface texture—**The
588 morphology and texture of the marginal dentition in therocephalians has only been discussed
589 anecdotally, but may provide important information regarding the interrelationships of
590 therocephalians, in addition to their diets (Huttenlocker et al., 2015). All eutherocephalians have
591 lost the serrations on the canines and antecanine teeth, but few eutherocephalians may have
592 retained smooth anterior and/or posterior carinae (e.g., chthonosaurids, some akidnognathids). In
593 some Permian eutherocephalians, the incisors and precanines may bear longitudinal fluting (e.g.,
594 basal akidnognathids, whaitsioids, and ictidosuchid-grade baurioids) or large, flat facets (derived
595 akidnognathids). Incisor fluting was suggested to be plesiomorphic for Eutherocephalia by
596 Hopson and Barghusen (1986), although the postcanine enamel texture was not discussed in any
597 detail. The condition of the incisors in *Ophidostoma* is unknown, but the presence of enamel
598 striae on the postcanines strongly suggests that striated postcanine enamel was also

599 plesiomorphic for the postcanines of early Eutherocephalia and its subclades, given its shared
600 presence in *Ophidostoma*, *Akidnognathus*, and *Ictidosuchus*. Incidentally, enamel fluting has also
601 been reported in the marginal dentition of the enigmatic scylacosaurian *Scylacosuchus* from
602 Russia (Ivakhnenko, 2011). Contrary to the recent suggestion of Huttenlocker et al. (2015:fig. 6)
603 that basal akidnognathids and ictidosuchid-grade baurioids evolved postcanine striae
604 independently, the new evidence from *Ophidostoma* suggests that a single evolutionary origin is
605 more parsimonious, followed by multiple losses of enamel fluting/striae on the antecanine teeth
606 and postcanines in derived Akidnognathidae, Whaitsioidea, and Baurioidea.
607
608 **Diversification of Therapsids during the End-Guadalupian Extinction**
609 Non-marine vertebrate diversifications and extinctions are poorly understood during the
610 middle-to-late Permian transition. Particularly, whereas most workers recognize marked
611 extinctions of entire groups by the end of the Guadalupian (e.g., dinocephalians, lycosuchids,
612 scylacosaurids), there is little consensus as to whether the proliferation of late Permian therapsid
613 assemblages during Wuchiapingian times constitutes survival and opportunistic expansion of
614 ecospace by pre-existing lineages (long-fuse) or a rapid radiation of new lineages (short-fuse)
615 during the extinction's aftermath (Fröbisch, 2008, 2013; Lucas, 2017). For example, Lucas
616 (2017) most recently characterized the extinction of dinocephalian faunas as an abrupt "global
617 event" (p. 55), although systematic paleontological collecting in the middle Permian
618 *Tapinocephalus* and *Pristerognathus* AZs suggests the turnover was more complex, and that the
619 apparent severity of dinocephalian extinctions is exaggerated by oversplit dinocephalian
620 taxonomy and poor temporal resolution (Rubidge et al., 2013; Day et al., 2015a,b). Nevertheless,
621 others have identified shifts in overall extinction rates of some post-Guadalupian therapsid

622 lineages—a potential driver of apparent (raw) diversity shifts in some Wuchiapingian lineages
623 (Brocklehurst et al., 2015)—while others still have raised doubts about the quality of the fossil
624 record and its ability to resolve the magnitude of turnover of middle-to-late Permian assemblages
625 (Fröbisch, 2008, 2013; Irmis et al., 2013).

626 We suggest that the apparent turnover of therocephalians can be characterized by a long-
627 fuse model in which classic late Permian clades (e.g., whaitsioids, baurioids) originated
628 concurrently with basal therocephalians of the middle Permian, but at lower abundances. This
629 hypothesis is supported by renewed collecting efforts in the Teekloof Formation by one of us
630 (RMHS), helping to further clarify therapsid ecological turnover during this time. Firstly, the
631 new record of *Microwhaitsia* represents one of the oldest known Gondwanan whaitsiids, as other
632 whaitsiid records from southern Africa are typically confined to the uppermost *Cistecephalus*
633 and lower *Daptocephalus* AZs (Huttenlocker and Abdala, 2015). *Microwhaitsia* firmly
634 establishes that whaitsiids already exhibited a Pangean-wide distribution by *Tropidostoma* AZ
635 times (early Wuchiapingian), an observation that is consistent with the record of the closely
636 allied *Viatkosuchus* from the Capitanian or Wuchiapingian-aged Kotelnich assemblage of Russia
637 (Golubev, 2000; Benton et al., 2012) (Fig. 11). Secondly, long-term collecting efforts by one of
638 us (RMHS) to elucidate the assemblages of the different members of the Teekloof Formation
639 have produced additional whaitsioid and baurioid records (see Tables 2 and 3). Some of these—
640 including a hofmeyriid (SAM-PK-K10525) (Fig. 12), an indeterminate ictidosuchid-grade
641 baurioid (SAM-PK-K6886) and a second baurioid with possible affinities to *Ictidosuchoides*
642 (SAM-PK-K11319)—were collected from the lower Poortjie Member or equivalent beds, which
643 contains a *Pristerognathus* AZ fauna that corresponds to either the latest Capitanian or earliest
644 Wuchiapingian global stages (Fig. 1).

Origination, extinction, and diversification rate shifts in therocephalians have been summarized elsewhere in the context of the Permo-Triassic mass extinction (Huttenlocker et al., 2011; Huttenlocker, 2013, 2014). For example, Huttenlocker (2014) failed to identify evidence of diversification rate shifts in small-bodied therocephalian lineages near the Permo-Triassic boundary, but noted a significant shift associated with the earlier divergence of the Eutherocephalia clade. This was attributed to either increasing origination rates of eutherocephalians or to sampling bias in the *Tropidostoma* and *Cistecephalus* AZs where therocephalian fossils are more abundant (Smith et al., 2012). More recently, Brocklehurst et al. (2015) showed that uneven origination and extinction rates (particularly elevated extinction) could be a driver of diversification rate shifts in Permo-Triassic tetrapods. Notably, both origination and extinction rates of therocephalians rose steadily into the late Permian (Fig. 11), despite the long lineage durations sustained by a few representative taxa during the Wuchiapingian (e.g., *Ictidosuchoides*, some hofmeyriids). In this sense, origination/extinction rates indicate that therocephalians (particularly eutherocephalians) were, on the whole, resilient to the effects of the extinction, although this was dependent upon high rates of turnover and replacement by individual genera. Unlike some baurioid lineages, whaitsioids became wholly extinct prior to the Permo-Triassic boundary as therocephalian origination rates began to markedly decrease. The reasons for this differential extinction remain unclear, but have been linked to differences in life history strategies evident in the two groups (Huttenlocker and Botha-Brink, 2013, 2014; Botha et al., 2016). Consequently, future collecting of precious middle-to-late Permian specimens will be crucial to further resolve the evolutionary dynamics of therocephalians spanning the end-Guadalupian and Permo-Triassic mass extinctions.

668 CONCLUSIONS

669

670 The new records of *Microwhaitsia* and *Ophidostoma* from the Teekloof Formation shed
671 light on the early evolution of eutherocephalians during the middle-to-late Permian transition.
672 Phylogenetic analysis recovers both of the new taxa within Whaitsioidea, with *Microwhaitsia* as
673 an early whaitsiid and *Ophidostoma* as an aberrant whaitsioid outside the hofmeyriid+whaitsiid
674 clade. Consequently, *Microwhaitsia* represents the oldest whaitsiid from Gondwana and, along
675 with additional early hofmeyriid and baurioid records, underscores the early dichotomy between
676 whaitsiid-line and baurioid-line therocephalians. Moreover, the disjunct geographic occurrences
677 of *Microwhaitsia* and *Viatkosuchus* suggest that whaitsiids already exhibited a cosmopolitan
678 distribution by the early Wuchiapingian. During the end-Guadalupian, the extinction of basal
679 lycosuchids and scylacosaurids was offset by increasing origination/extinction rates of
680 eutherocephalians, which flourished into Wuchiapingian times. As a part of this radiation,
681 whaitsioids represent a previously underappreciated but successful clade of late Permian
682 eutherocephalians, but they did not survive the ecological impacts of the Permo-Triassic mass
683 extinction. Future collecting will provide added resolution on the middle-to-late Permian
684 transition, and will further clarify the dynamic replacement of basal therocephalians
685 (lycosuchids, scylacosaurids) by eutherocephalians and other early-diverging therapsid predators
686 (gorgonopsians, cynodonts).

687

688 ACKNOWLEDGMENTS

689

For collections access, we thank S. Kaal and the Iziko South African Museum, Cape Town, and B. Rubidge and B. Zipfel of the Evolutionary Studies Institute (former Bernard Price Institute, BP), Johannesburg. For comments on SAM-PK-K8516 and help in the field, we thank S. Modesto. CT scans of SAM-PK-K8516 were produced by the University of Utah Core Imaging Facility, Salt Lake City.

## REFERENCES

Abdala, F. 2007. Redescription of *Platycraniellus elegans* (Therapsida, Cynodontia) from the Lower Triassic of South Africa, and the cladistic relationships of eutheriodonts. Palaeontology 50:591–618.

Abdala, F., T. Jashashvili, B. S. Rubidge, and J. van den Heever. 2014. New material of *Microgomphodon oligocynus* (eutherapsida, therocephalia) and the taxonomy of southern african bauriidae, p. 209–231 in C. F. Kammerer, K. D. Angielczyk, and J. Fröbisch (eds.) Early Evolutionary History of the Synapsida. Springer, Dordrecht.

Abdala, F., C. F. Kammerer, M. O. Day, S. Jirah, and B. S. Rubidge. 2014. Adult morphology of the therocephalian *Simorhinella baini* from the middle Permian of South Africa and the taxonomy, paleobiogeography, and temporal distribution of the Lycosuchidae. Journal of Paleontology 88:1139–1153.

Abdala, F., B. S. Rubidge, and J. van den Heever. 2008. The oldest therocephalians (Therapsida, Eutheriodontia) and the early diversification of Therapsida. Palaeontology 51:1011–1024.

711 Attridge, J. 1956. The morphology and relationships of a complete therocephalian skeleton from
712 the *Cistecephalus* Zone of South Africa. Proceedings of the Royal Society of Edinburgh.
713 Section B 66:59–93.
714 Benton, M. J., A. J. Newell, G. D. Price, and A. A. Kurkin. 2012. Preservation of exceptional
715 vertebrate assemblages in Middle Permian fluviolacustrine mudstones of Kotel'nich,
716 Russia: stratigraphy, sedimentology, and taphonomy. Palaeogeography,
717 Palaeoclimatology, Palaeoecology 319:58–83.
718 Botha, J., F. Abdala, and R. Smith. 2007. The oldest cynodont: new clues on the origin and early
719 diversification of Cynodontia. Zoological Journal of the Linnean Society 149:477–492.
720 Botha-Brink, J., D. Codron, A. K. Huttenlocker, K. D. Angielczyk, and M. Ruta. 2016. Breeding
721 young as a survival strategy during Earth's greatest mass extinction. Scientific Reports
722 6:24053.
723 Brink, A. S. 1956. On *Aneugomphius ictidoceps* Broom & Robinson. Palaeontologia Africana
724 4:97–115.
725 Brink, A. S. 1980. On the genus *Theriognathus* Owen (including *Whaitsia*, *Notosollasia*,
726 *Alopecopsis*, *Notaelurops*, *Moschorhynchus* and *Aneugomphius*). Annals of the
727 Geological Survey of South Africa 14:1–37.
728 Brocklehurst, N., M. Ruta, J. Müller, and J. Fröbisch. 2015. Elevated extinction rates as a trigger
729 for diversification rate shifts: early amniotes as a case study. Scientific Reports 5:17104.
730 Broom, R. 1911. On some new South African Permian reptiles. Proceedings of the Zoological
731 Society of London 81:1073–1082.
732 Broom, R. 1935. On some new genera and species of Karroo fossil reptiles. Annals of the
733 Transvaal Museum 18:55–72.

734 Broom, R. 1948. A contribution to our knowledge of the vertebrates of the Karoo beds of South
735 Africa. Transactions of the Royal Society of Edinburgh 61:577–629.
736 Cole, D. I. 1992. Evolution and development of the Karoo Basin, Pp. 87-99 in M.J. De Wit &
737 I.G.D. Ransome (eds.), Inversion Tectonics of the Cape Fold Belt, Karoo and Cretaceous
738 Basins of Southern Africa, A.A. Balkema, Rotterdam.
739 Crompton, A. W. 1955. A revision of the scaloposauridae with special reference to kinetism in
740 this family. Navorsinge Van Die Nasionale Museum 1:149–183.
741 Day, M. O., S. Güven, F. Abdala, S. Jirah, B. Rubidge, and J. Almond. 2015a. Youngest
742 dinocephalian fossils extend the *Tapinocephalus* Zone, Karoo Basin, South Africa. South
743 African Journal of Science 111:1–5.
744 Day, M. O., J. Ramezani, S. A. Bowring, P. M. Sadler, D. H. Erwin, F. Abdala, and B. S.
745 Rubidge. 2015b. When and how did the terrestrial mid-Permian mass extinction occur?
746 Evidence from the tetrapod record of the Karoo Basin, South Africa. *Proc. R. Soc. B*
747 282(1811):20150834.
748 Fröbisch, J. 2008. Global taxonomic diversity of anomodonts (Tetrapoda, Therapsida) and the
749 terrestrial rock record across the Permian-Triassic boundary. PLoS One 3(11):e3733.
750 Fröbisch, J. 2013. Vertebrate diversity across the end-Permian mass extinction—Separating
751 biological and geological signals. Palaeogeography, Palaeoclimatology, Palaeoecology
752 372:50–61.
753 Golubev, V. K. 2000. The faunal assemblages of Permian terrestrial vertebrates from Eastern
754 Europe. Paleontological Journal 34(suppl. 2):S211–S224.
755 Haughton, S. H. 1918. Some new carnivorous Therapsida, with notes upon the braincase in
756 certain species. Annals of the South African Museum 12:175–216.

757 Heever, J. A. van den. 1994. The cranial anatomy of the early Therocephalia (Amniota:
758 Therapsida). Annals of the University of Stellenbosch 1:1–59.
759 Hillenius, W. J. 1994. Turbinates in therapsids: evidence for Late Permian origins of mammalian
760 endothermy. Evolution 48:207–229.
761 Hopson, J. A., and H. R. Barghusen. 1986. An analysis of therapsid relationships. Pp. 83–106 in
762 N. Hotton, P. D. MacLean, J. J. Roth, and E. C. Roth (eds.) The Ecology and Biology of
763 Mammal-like Reptiles. Smithsonian Institution Press, Washington.
764 Huttenlocker, A. K. 2009. An investigation into the cladistic relationships and monophyly of
765 therocephalian therapsids (Amniota: Synapsida). Zoological Journal of the Linnean
766 Society 157:865–891.
767 Huttenlocker, A. K. 2013. Paleobiology of therocephalian synapsids (Amniota) and the effects of
768 the end-Permian extinction on size, growth and bone microstructure. Ph.D. dissertation,
769 University of Washington, Seattle.
770 Huttenlocker, A. K. 2014. Body size reductions in nonmammalian eutheriodont therapsids
771 (Synapsida) during the end-Permian mass extinction. PLoS One 9:e87553.
772 Huttenlocker, A. K. and F. Abdala. 2015. Revision of the first therocephalian, *Theriognathus*
773 *microps* Owen (Therapsida: Whaitsiidae), and implications for cranial ontogeny and
774 allometry in nonmammalian eutheriodonts. Journal of Paleontology 89:645–664.
775 Huttenlocker, A. K., and J. Botha-Brink. 2013. Body size and growth patterns in the
776 therocephalian *Moschorhinus kitchingi* (Therapsida: Eutheriodontia) before and after the
777 end-Permian extinction in South Africa. Paleobiology 39:253–277.

778 Huttenlocker, A. K., and J. Botha-Brink. 2014. Bone microstructure and the evolution of growth
779 patterns in Permo-Triassic therocephalians (Amniota, Therapsida) of South Africa. PeerJ
780 2:e325.
781 Huttenlocker, A. K., and C. A. Sidor. 2012. Taxonomic revision of therocephalians (Therapsida:
782 Theriodontia) from the Lower Triassic of Antarctica. American Museum Novitates
783 3738:1–19.
784 Huttenlocker, A. K., and C. A. Sidor. 2016. The first karenitid (Therapsida, Therocephalia) from
785 the upper Permian of Gondwana and the biogeography of Permo-Triassic
786 therocephalians. Journal of Vertebrate Paleontology 36:e1111897.
787 Huttenlocker, A. K., C. A. Sidor, and K. D. Angielczyk. 2015. A new eutherocephalian
788 (Therapsida, Therocephalia) from the upper Permian Madumabisa Mudstone Formation
789 (Luangwa Basin) of Zambia. Journal of Vertebrate Paleontology 35:e969400.
790 Huttenlocker, A. K., C. A. Sidor, and R. M. H. Smith. 2011. A new specimen of
791 *Promoschorhynchus* (Therapsida: Therocephalia: Akidnognathidae) from the Lower
792 Triassic of South Africa and its implications for theriodont survivorship across the
793 Permo-Triassic boundary. Journal of Vertebrate Paleontology 31:405–421.
794 Irmis, R. B., J. H. Whiteside, and C. F. Kammerer. 2013. Non-biotic controls of observed
795 diversity in the paleontologic record: An example from the Permo-Triassic Karoo Basin
796 of South Africa. Palaeogeography, Palaeoclimatology, Palaeoecology 372:62–77.
797 Ivakhnenko, M. F. 2011. Permian and Triassic therocephals (Eutherapsida) of Eastern Europe.
798 Paleontological Journal 45:981–1144.
799 Kemp, T. S. 1972a. Whaitsiid Therocephalia and the origin of cynodonts. Philosophical
800 Transactions of the Royal Society of London: Series B 264:1-54.

801 Kemp, T.S. 1972b. The jaw articulation and musculature of the whaitsiid Therocephalia; pp.
802 213-230 in K.A. Joysey & T.S. Kemp (eds.), *Studies in Vertebrate Evolution.* Winchester
803 Press, New York, U.S.
804 Kemp, T. S. 2012. The origin and radiation of therapsids. pp. 2–28 in A. Chinsamy (ed.)
805 Forerunners of Mammals: Radiation, Histology, Biology. Indiana University Press,
806 Bloomington.
807 Lewis, P. O. 2001. A likelihood approach to estimating phylogeny from discrete morphological
808 character data. Systematic Biology 50:913–925.
809 Liu, J., and F. Abdala. 2017. Therocephalian (Therapsida) and chroniosuchian (Reptiliomorpha)
810 from the Permo-Triassic transitional Guodikeng Formation of the Dalongkou Section,
811 Jimsar, Xinjiang, China. Vertebrata PalAsiatica 55:24–40.
812 Lucas, S. G. 2017. Permian tetrapod extinction events. Earth-Science Reviews 170:31–60.
813 Mendrez, C. H. 1974a. Etude du crane d'un jeune specimen de *Moschorhinus kitchingi* Broom, 1920
814 (?*Tigrisuchus simus* Owen, 1876), Therocephalia, Pristerosauria, Moschorhinidae d'Afrique
815 Australe (Remarques sur les Moschorhinidae et les Whaitsiidae). Annals of the South
816 African Museum 64:71–115. [In French.]
817 Owen, R. 1876. Descriptive and Illustrated Catalogue of the Fossil Reptilia of South Africa in
818 the Collection of the British Museum. Printed by order of the Trustees, London.
819 Ronquist, F., P. van der Mark, and J. P. Huelsenbeck. 2009. Bayesian phylogenetic analysis
820 using MrBayes: Pp. 210–266 in A. M. Vandamme, M. Salemi, and P. Lemey (eds.) The
821 Phylogenetic Handbook 2nd Edition. Cambridge University Press, Cambridge.
822 Rosset, A., L. Spadola, and O. Ratib. 2004. OsiriX: An open-source software for navigating in
823 multidimensional DICOM images. J. Digit. Imaging 17.

824 Rubidge, B. S., D. H. Erwin, J. Ramezani, S. A. Bowring, and W. J. de Klerk. 2013. High-
825 precision temporal calibration of late Permian vertebrate biostratigraphy: U-Pb zircon
826 constraints from the Karoo Supergroup, South Africa. Geology 41:363–366.
827 Sidor, C.A., D. A. Vilhena, K. D. Angielczyk, A. K. Huttenlocker, S. J. Nesbitt, B. R. Peecook,
828 J. S. Steyer, R. M. H. Smith and L. A. Tsuji. 2013. Provincialization of terrestrial faunas
829 following the end-Permian mass extinction. Proceedings of the National Academy of
830 Sciences 110:8129–8133.
831 Sigurdsen, T. 2006. New features of the snout and orbit of a therocephalian therapsid from South
832 Africa. Acta Palaeontologica Polonica 51:63–75.
833 Sigurdsen, T., A. K. Huttenlocker, S. P. Modesto, T. B. Rowe, and R. Damiani. 2012.
834 Reassessment of the morphology and paleobiology of the therocephalian *Tetracynodon*
835 *darti* (Therapsida), and the phylogenetic relationships of Baurioidea. Journal of
836 Vertebrate Paleontology 32:1113–1134.
837 Smith, R. M. H. 1987. Morphology and depositional history of exhumed Permian point bars in
838 the southwestern Karoo, South Africa. Journal Sedimentary Petrology 57:19-29.
839 Smith, R. M. H. 1990. Alluvial paleosols and pedofacies sequences in the Permian Lower
840 Beaufort of the southwestern Karoo Basin, South Africa. Journal Sedimentary Petrology
841 60:258-276
842 Smith, R. M. H. 1993. Vertebrate taphonomy of Late Permian floodplain deposits in the
843 southwestern Karoo Basin of South Africa. Palaios 8:45–67.
844 Smith, R.M. H., and J. Botha-Brink. 2011. Morphology and composition of bone-bearing
845 coprolites from the Late Permian Beaufort Group, Karoo Basin, South Africa.
846 Palaeogeography, Palaeoclimatology, Palaeoecology 312:40–53.

847 Smith, R. M. H., B. Rubidge, and M. van der Walt. 2012. Therapsid biodiversity patterns and
848 paleoenvironments of the Karoo Basin, South Africa: pp. 30–62 in A. Chinsamy (ed.)
849 Forerunners of Mammals: Radiation, Histology, Biology. Indiana University Press,
850 Bloomington.
851 Swofford, D. 1999. PAUP* Phylogenetic analysis using parsimony v. 4.0 beta 10. Sinauer
852 Associates, Sunderland, MA.
853 Tatarinov, L. P. 1963. A new Late Permian therocephalian. Paleontological Journal 4:76–94.
854 Tatarinov, L. P. 1974. Theriodonts of the USSR. Trudy Paleontologicheskogo Instituta,
855 Akademii Nauk SSSR 143:1–240. [in Russian]
856 Tatarinov, L. P. 1995. *Viatkosuchus sumini*, a new Late Permian therocephalian from the Kirov
857 region. Paleontological Journal 29:111–128.
858 Turner, B. R. 1978. Sedimentary patterns of uranium mineralization in the Beaufort Group of the
859 southern Karoo (Gondwana) Basin, South Africa. In: A.D.Miall (Editor), Fluvial
860 Sedimentology, Canadian Association of Petroleum Geologists. Memoir 5:831–848.
861 Watson, D. M. S., and A. S. Romer. 1956. A classification of therapsid reptiles. Bulletin of the
862 Museum of Comparative Zoology, Harvard 111:37–89.
863
864
865
866
867
868
869
870

871 FIGURE & TABLE LEGENDS

872

873 FIGURE 1. Specimen provenance and stratigraphic context of Teekloof Formation whaitsioids.
874 1, Provenance of SAM-PK-K10990 and K10984, Badshoek farm (De Hoop 117), near Beaufort
875 West, Western Cape Province; 2, Provenance of SAM-PK- K8516, Good Luck farm, near
876 Fraserburg, Northern Cape Province. Bulleted numbers to right of stratigraphic column indicate
877 ages of vertebrate assemblage zones in millions of years (**Ma**) (from Rubidge et al., 2013).
878 Geologic map modified from Smith (1993). **Abbreviations**: ***Ci*AZ**, *Cistecephalus* Assemblage
879 Zone; ***Dapto*AZ**, *Daptocephalus* Assemblage Zone; **Fm**, Formation; **M**, Member; ***Prist*AZ**,
880 *Pristerognathus* Assemblage Zone; ***Tapino*AZ**, *Tapinocephalus* Assemblage Zone; ***Tr*AZ**,
881 *Tropidostoma* Assemblage Zone. [full page width]

882

883 FIGURE 2. Holotypic skull of *Microwhaitsia mendrezi* gen. et sp. nov. (SAM-PK-K10990) in
884 dorsal (**A**), ventral (**B**), and right lateral (**C**) views. [full page width]

885

886 FIGURE 3. Interpretive line drawings of the holotypic skull of *Microwhaitsia mendrezi* gen. et
887 sp. nov. (SAM-PK-K10990) in dorsal (**A**), ventral (**B**), and right lateral (**C**) views.
888 **Abbreviations**: **d**, dentary; **C**, upper canine; **cr.ch**, crista choanalis; **f**, frontal; **f.l**, lacrimal
889 foramen; **I5**, fifth upper incisor; **j**, jugal; **l**, lacrimal; **m**, maxilla; **n**, nasal; **p**, parietal; **pal**,
890 palatine; **pC**, upper precanine; **PC5**, fifth upper postcanine; **po**, postorbital; **pm**, premaxilla; **prf**,
891 prefrontal; **pt**, pterygoid; **sa**, surangular; **sm**, septomaxilla; **sp**, splenial. [full page width]

892

FIGURE 4. Stereopair images of the palate of the holotypic skull of *Microwhaitsia mendrezi* gen. et sp. nov. (SAM-PK-K10990) in left oblique ventral (**A**) and posteroventral (**B**) views. Note the narrow contact between the left crista choanalis and vomer without sutural connection. [two-thirds page width]

FIGURE 5. Referred specimen of *Microwhaitsia mendrezi* gen. et sp. nov. (SAM-PK-K10984) in dorsal (**A**), ventral (**B**), and left lateral (**C**) views. [one column's width]

FIGURE 6. Interpretive line drawings of referred specimen of *Microwhaitsia mendrezi* gen. et sp. nov. (SAM-PK-K10984) in dorsal (**A**), ventral (**B**), and left lateral (**C**) views. **Abbreviations**: **C**, upper canine alveolus; **cr.ch**, crista choanalis; **ect**, ectopterygoid; **f**, frontal; **j**, jugal; **l**, lacrimal; **m**, maxilla; **m.pal.f**, maxillo-palatine foramen; **n**, nasal; **pal**, palatine; **PC5**, fifth upper postcanine alveolus; **prf**, prefrontal; **pt**, pterygoid; **v**, vomer; **v.suborb**, suborbital vacuity. [one column's width]

FIGURE 7. Volumized HRXCT scans of the skull of *Ophidostoma tatarinovi* gen. et sp. nov. (SAM-PK-K8516) in dorsal (**A**), ventral (**B**), left lateral (**C**), and frontal (**D**) views. [full page width]

FIGURE 8. Interpretive line drawings of the skull of *Ophidostoma tatarinovi* gen. et sp. nov. (SAM-PK-K8516) in dorsal (**A**), ventral (**B**), left lateral (**C**), and frontal (**D**) views. **Abbreviations**: **a**, angular; **d**, dentary; **ect**, ectopterygoid; **c**, lower canine; **C**, upper canine; **f**, frontal; **fen.m**, mandibular fenestra; **i**, lower incisor; **j**, jugal; **l**, lacrimal; **m**, maxilla; **n**, nasal; **p**,

parietal; **part**, prearticular; **pbs**, para-basisphenoid; **PC6**, sixth upper postcanine; **po**, postorbital; **pm**, premaxilla; **prf**, prefrontal; **pt**, pterygoid; **q-qj**, quadrate-quadratojugal complex; **sa**, surangular; **sm**, septomaxilla; **sp**, splenial; **sq**, squamosal; **v.ipt**, interpterygoid vacuity; **v.suborb**, suborbital vacuity. [full page width]

FIGURE 9. Conservative phylogenetic relationships of the major clades of eutherocephalians, showing conflicting arrangements obtained from Bayesian and parsimony analyses as polytomies (tree length = 381; consistency index (CI) = 0.438; retention index = 0.789; rescaled CI = 0.346).

FIGURE 10. New specimen of the hofmeyriid *Mirotenthes digitipes* Attridge, 1956 (SAM-PK-K11188) from the upper *Cistecephalus* Assemblage Zone of 'Good Luck.' Specimen shown in dorsal oblique view, showing the large temporal fenestra and broad, anvil-shaped epipterygoid (**ept**) processus ascendens. [two-thirds page width]

FIGURE 11. Stratigraphically calibrated phylogeny of middle Permian through Triassic therocephalians showing calibration points for minimum divergence dates of major clades (**A**). Light gray lines represent hypothetical phylogenetic branching, whereas black bars represent observed stratigraphic ranges (dashed ends indicate taxa having unknown upper or lower ranges). Graph (**B**) shows peak levels of eutherocephalian origination/extinction by the Wuchiapingian stage. **Abbreviations**: **An**, Antarctica; **Ch**, China; **Chx**, Changxingian; ***Ci*AZ**, *Cistecephalus* Assemblage Zone; ***Dapto*AZ**, *Daptocephalus* Assemblage Zone; **Ind**, Induan; **Na**, Namibia; **Olen**, Olenekian; ***Prist*AZ**, *Pristerognathus* Assemblage Zone; **Roa**, Roadian; **Ru**,

938 Russia; **SA**, South Africa; ***Tapino*AZ**, *Tapinocephalus* Assemblage Zone; ***Tr*AZ**, *Tropidostoma*
939 Assemblage Zone; **Tz**, Tanzania; **Wor**, Wordian; **Za**, Zambia. [full page]
940
941 FIGURE 12. Representative hofmeyriid from the late Capitanian or earliest Wuchiapingian of
942 the Karoo Basin, South Africa, compared to other known specimens of *Hofmeyria*. SAM-PK-
943 K10525 (**A**), Hofmeyriidae from the *Pristerognathus* Assemblage Zone of Lombardskraal,
944 Beaufort West district, Western Cape Province. Specimen shows short, high rostrum, prefrontal-
945 postorbital contact in orbit, anteriorly expanded epipterygoid, and conical, non-serrated/non-
946 carinated maxillary teeth. BP/1/4404 (BP, former Bernard Price Institute, now Evolutionary
947 Studies Institute, Johannesburg) (**B**), *Hofmeyria* cf. *H. atavus* from the *Cistecephalus*
948 Assemblage Zone of Matjiesfontein (Highlands), Victoria West district, Northern Cape Province.
949 BP/1/1399 (**C**), *Hofmeyria* cf. *H. atavus* from the *Cistecephalus* Assemblage Zone of
950 Driehoeksfontein, Murraysburg district, Western Cape Province. Numbers 14–136 are characters
951 listed in the phylogenetic analysis (see online Supplemental Appendix) followed by the derived
952 state in parentheses corresponding to hofmeyriids or other early whaitsioids. **Abbreviations**:
953 **AZ**, Assemblage Zone; **PC**, postcanine position #. [full page]
954
955 TABLE 1. List of tetrapod fossils collected from the two farms ‘Badshoek’ and ‘Good Luck’ by
956 the Iziko South African Museum between 1996 and 2015. The newly described therocephalian
957 species are bold.
958
959 TABLE 2. African Permo-Triassic therocephalians by Karoo assemblage zone or equivalent
960 (updated from Abdala et al., 2008 and Huttenlocker, 2013).

961

962 TABLE 3. Russian and Chinese Permo-Triassic therocephalians by assemblage zone or stage

963 (updated from Abdala et al., 2008, Ivakhnekno, 2011, and Huttenlocker, 2013).

964

965

## Table 1(on next page)

Table 1

List of tetrapod fossils collected from the two farms ‘Badshoek’ and ‘Good Luck’ by the Iziko South African Museum between 1996 and 2015. The newly described therocephalian species are bold.

**Table 1.** List of tetrapod fossils collected from the two farms 'Badshoek' and 'Good Luck' by the Iziko South African Museum between 1996 and 2015. The newly described therocephalian species are bold.

| Specimen Number | Identification | Stratigraphic Level |
|---|---|---|
| **Good Luck (Matjiesfontein 412)** | | |
| SAM-PK-K11279 | *Dicynodon* sp. | Steenkamp member (lower *Dapto*AZ) |
| SAM-PK-K11189 | *Cistecephalus microrhinus* | Oukloof/Steenkamp (uppermost *Ci*AZ) |
| SAM-PK-K11188 | *Mirotenthes digitipes* | Oukloof/Steenkamp (uppermost *Ci*AZ) |
| SAM-PK-K8630 | *Pareiasaurus* sp. | Oukloof member (upper *Ci*AZ) |
| SAM-PK-K8508 | *Diictodon* sp. | Oukloof member (upper *Ci*AZ) |
| SAM-PK-K8509 | *Diictodon* sp. | Oukloof member (upper *Ci*AZ) |
| SAM-PK-K8513 | *Diictodon* sp. | Oukloof member (upper *Ci*AZ) |
| SAM-PK-K8303 | *Cistecephalus* sp. | Oukloof member (upper *Ci*AZ) |
| SAM-PK-K8304 | *Cistecephalus* sp. | Oukloof member (upper *Ci*AZ) |
| SAM-PK-K8510 | *Cistecephalus* sp. | Oukloof member (upper *Ci*AZ) |
| SAM-PK-K8512 | *Cistecephalus* sp. | Oukloof member (upper *Ci*AZ) |
| SAM-PK-K8629 | *Cistecephalus* sp. | Oukloof member (upper *Ci*AZ) |
| SAM-PK-K11187 | *Cistecephalus* sp. | Oukloof member (upper *Ci*AZ) |
| SAM-PK-K8307 | *Oudenodon* sp. | Oukloof member (upper *Ci*AZ) |
| SAM-PK-K11280 | *Oudenodon* sp. | Oukloof member (upper *Ci*AZ) |
| SAM-PK-K8507 | *Dicynodon* sp. | Oukloof member (upper *Ci*AZ) |
| SAM-PK-K8516 | ***Ophidostoma tatarinovi*** (type) | Oukloof member (upper *Ci*AZ) |
| SAM-PK-K8631 | Eutherocephalia indet. | Oukloof member (upper *Ci*AZ) |
| SAM-PK-K8511 | *Procynosuchus delaharpeae* | Oukloof member (upper *Ci*AZ) |
| SAM-PK-K11186 | *Procynosuchus delaharpeae* | Oukloof member (upper *Ci*AZ) |
| **Badshoek (De Hoop 117)** | | |
| SAM-PK-K10449 | *Pristerodon* sp. | Oukloof member (*Ci*AZ) |
| SAM-PK-K11008 | *Pristerodon* sp. | Hoedemaker member (upper *Tr*AZ) |
| SAM-PK-K11009 | *Pristerodon* sp. | Hoedemaker member (upper *Tr*AZ) |
| SAM-PK-K11010 | *Pristerodon* sp. | Hoedemaker member (upper *Tr*AZ) |
| SAM-PK-K11011 | *Diictodon* sp. | Hoedemaker member (upper *Tr*AZ) |
| SAM-PK-K10987 | *Pristerodon* sp. | Hoedemaker member (*Tr*AZ) |
| SAM-PK-K10985 | *Diictodon* sp. | Hoedemaker member (*Tr*AZ) |
| SAM-PK-K10986 | *Emydops* sp. | Hoedemaker member (*Tr*AZ) |
| SAM-PK-K11000 | *Tropidostoma* sp. | Hoedemaker member (*Tr*AZ) |
| SAM-PK-K10983 | Gorgonopsia indet. | Hoedemaker member (*Tr*AZ) |
| SAM-PK-K10984 | ***Microwhaitsia mendrezi*** | Hoedemaker member (*Tr*AZ) |
| SAM-PK-K10990 | ***Microwhaitsia mendrezi*** (type) | Hoedemaker member (*Tr*AZ) |

*Ci*AZ, *Cistecephalus* Assemblage Zone; *Dapto*AZ, *Daptocephalus* Assemblage Zone; *Tr*AZ, *Tropidostoma* Assemblage Zone.

## Table 2(on next page)

Table 2

African Permo-Triassic therocephalians by Karoo assemblage zone or equivalent (updated from Abdala et al., 2008 and Huttenlocker, 2013).

**Table 2.** African Permo-Triassic therocephalians by Karoo assemblage zone or equivalent (updated from Abdala et al., 2008 and Huttenlocker, 2013).

**Permian**

*Eodicynodon* Assemblage Zone (Wordian) (2)
- *Glanosuchus macrops*
- *Ictidosaurus angusticeps*

*Tapinocephalus* Assemblage Zone (Capitanian) (8)
- *Alopecodon priscus*
- *Blattoidealestes gracilis**
- *Crapartinella croucheri**
- *Glanosuchus macrops*
- *Ictidosaurus angusticeps*
- *Lycosuchus vanderrieti*
- *Pardosuchus whaitsi*
- *Pristerognathus polyodon*
- *Scylacosaurus sclateri*
- *Simorhinella baini*

*Pristerognathus* Assemblage Zone (late Capitanian–Wuchiapingian) (5)
- *Glanosuchus macrops*
- Hofmeyriidae (cf. *Hofmeyria*)
- Ictidosuchidae (cf. *Ictidosuchoides*)
- *Lycosuchus vanderrieti*
- *Pristerognathus polyodon*

*Tropidostoma* Assemblage Zone (Wuchiapingian) (6)
- *Choerosaurus dejageri*
- *Hofmeyria atavus*
- *Ictidostoma hemburyi*
- *Ictidosuchoides longiceps*
- *Ictidosuchus primaevus*
- *Microwhaitsia mendrezi*

*Cistecephalus* Assemblage Zone (Wuchiapingian) (8)
- *Mupashi migrator*
- *Euchambersia mirabilis*
- *Hofmeyria atavus*
- *Ichibengops munyamadziensis*
- *Ictidostoma hemburyi*
- *Ictidosuchoides longiceps*
- *Mirotenthes digitipes*
- *Ophidostoma tatarinovi*
- *Polycynodon elegans*
- *Theriognathus microps*
- Unnamed akidnognathid (USNM PAL 412421)

*Daptocephalus* Assemblage Zone (Wuchiapingian–Changxingian) (11)
- *Akidnognathus parvus*
- *Cerdosuchoides brevidens*
- *Ictidochampsa platyceps*
- *Ictidosuchoides longiceps*
- *Ictidosuchops rubidgei*
- *Lycideops longiceps*

*Mirotenthes digitipes*
*Moschorhinus kitchingi*
*Promoschorhynchus platyrhinus*
*Tetracynodon tenuis*
*Theriognathus microps*

**Triassic**
*Lystrosaurus* Assemblage Zone (Induan–Olenekian) (7)
*Ericiolacerta parva*
*Moschorhinus kitchingi*
*Olivierosuchus parringtoni*
*Promoschorhynchus* cf. *P. platyrhinus* †
*Regisaurus jacobi*
*Scaloposaurus constrictus*
*Tetracynodon darti*
*Cynognathus* Assemblage Zone (Olenekian–Anisian) (2)
*Bauria cynops*
*Microgomphodon oligocynus*

* Taxa denoted by asterisk are considered invalid or based on non-diagnostic juvenile material;
†SAM-PK-K10014, originally identified as *Ictidosuchoides* (Smith and Botha, 2005; Botha and Smith, 2006; Abdala et al., 2008; Huttenlocker et al., 2011)

## Table 3(on next page)

Table 3

Russian and Chinese Permo-Triassic therocephalians by assemblage zone or stage (updated from Abdala et al., 2008, Ivakhnekno, 2011, and Huttenlocker, 2013).

**Table 3**. Russian and Chinese Permo-Triassic therocephalians by assemblage zone or stage (updated from Abdala et al., 2008, Ivakhnekno, 2011, and Huttenlocker, 2013).

**Permian**

Wordian–Capitanian (*Ulemosaurus* Assemblage Zone, Isheevo fauna or equivalent) (2)
- *Perplexisaurus*(?) *lepusculus**
- *Porosteognathus efremovi*

late Capitanian–Wuchiapingian? (*Deltavjatia* Assemblage Zone, Kotelnich fauna or equivalent) (6)
- *Karenites ornamentatus*
- *Kotelcephalon viatkensis*
- *Perplexisaurus* (=*Chlynovia*) *foveatus*
- *Scalopodon tenuisfrons*
- *Scalopodontes kotelnichi*
- *Viatkosuchus sumini*

Wuchiapingian (*Proelginia* Assemblage Zone, Ilynskoe fauna or equivalent) (1)
- *Scylacosuchus orenburgensis*

Wuchiapingian-Changxingian? (*Scutosaurus* Assemblage Zone, Sokolki fauna or equivalent) (2)
- *Annatherapsidus petri*
- *Chthonosaurus velocidens*

Changxingian (*Archosaurus* Assemblage Zone, Vyazniki fauna or equivalent) (6)
- *Dalongkoua fuae*†
- *Hexacynodon purlinensis**
- *Malasaurus germanus**
- *Moschowhaitsia vjuschkovi*
- *Purlovia maxima*
- Whaitsiidae indet.

**Triassic**

Induan–Olenekian (Vetlugian stage or equivalent) (5)
- *Hazhenia concava*
- *Scalopognathus multituberculatus**
- *Silphedosuchus orenburgensis*
- *Urumchia lii*
- *Yikezhaogia megafenestrala*

Anisian (*Eryosuchus* Assemblage Zone, Donguzian fauna or equivalent) (7)
- *Antecosuchus ochevi*
- *Dongusaurus schepetovi*†
- *Nothogomphodon danilovi*
- *Nothogomphodon sanjiaoensis*
- *Ordosiodon lincheyuensis*
- *Ordosiodon youngi*
- *Traversodontoides wangwuensis*

* Taxa denoted by asterisk are considered invalid or based on non-diagnostic material

† Precise age uncertain. Regarded as Permo-Triassic by Liu and Abdala, 2017.

# Figure 1

Specimen provenance and stratigraphic context of Teekloof Formation whaitsioids.

1, Provenance of SAM-PK-K10990 and K10984, Badshoek farm (De Hoop 117), near Beaufort West, Western Cape Province; 2, Provenance of SAM-PK- K8516, Good Luck farm, near Fraserburg, Northern Cape Province. Bulleted numbers to right of stratigraphic column indicate ages of vertebrate assemblage zones in millions of years (**Ma**) (from Rubidge et al., 2013). Geologic map modified from Smith (1993). **Abbreviations**: ***Ci*AZ**, *Cistecephalus* Assemblage Zone; ***Dapto*AZ**, *Daptocephalus* Assemblage Zone; **Fm**, Formation; **M**, Member; ***Prist*AZ**, *Pristerognathus* Assemblage Zone; ***Tapino*AZ**, *Tapinocephalus* Assemblage Zone; ***Tr*AZ**, *Tropidostoma* Assemblage Zone.

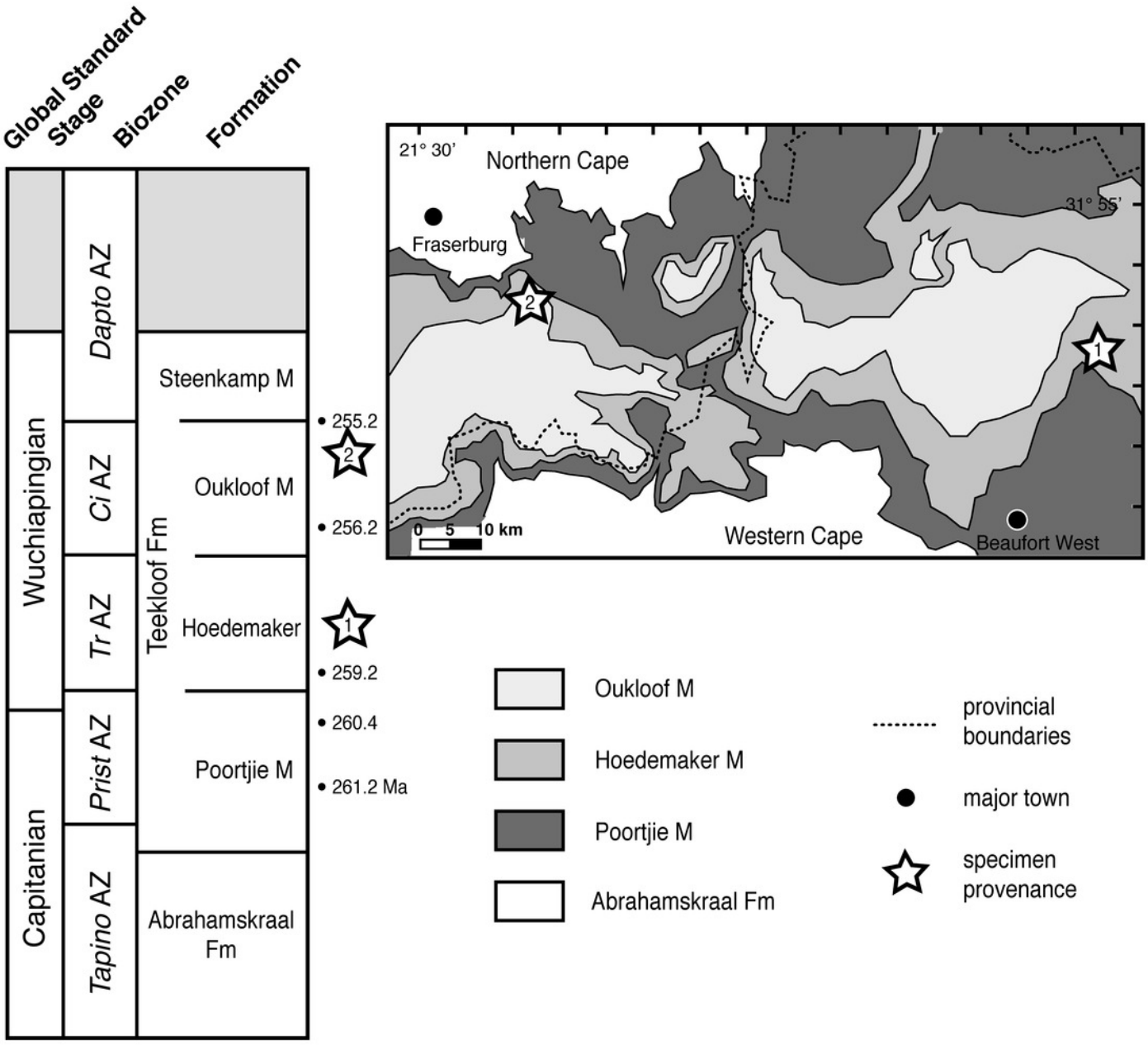
Global Standard Stage
Biozone
Formation
Wuchiapingian
Capitanian
Dapto AZ
Ci AZ
Tr AZ
Prist AZ
Tapino AZ
Teekloof Fm
Steenkamp M
Oukloof M
Hoedemaker
Poortjie M
Abrahamskraal Fm
255.2
256.2
259.2
260.4
261.2 Ma
21° 30'
Northern Cape
31° 55'
Fraserburg
Western Cape
Beaufort West
0 5 10 km
Oukloof M
Hoedemaker M
Poortjie M
Abrahamskraal Fm
provincial boundaries
major town
specimen provenance

# Figure 2

Holotypic skull of *Microwhaitsia mendrezi* gen. et sp. nov. (SAM-PK-K10990) in dorsal (A), ventral (B), and right lateral (C) views.

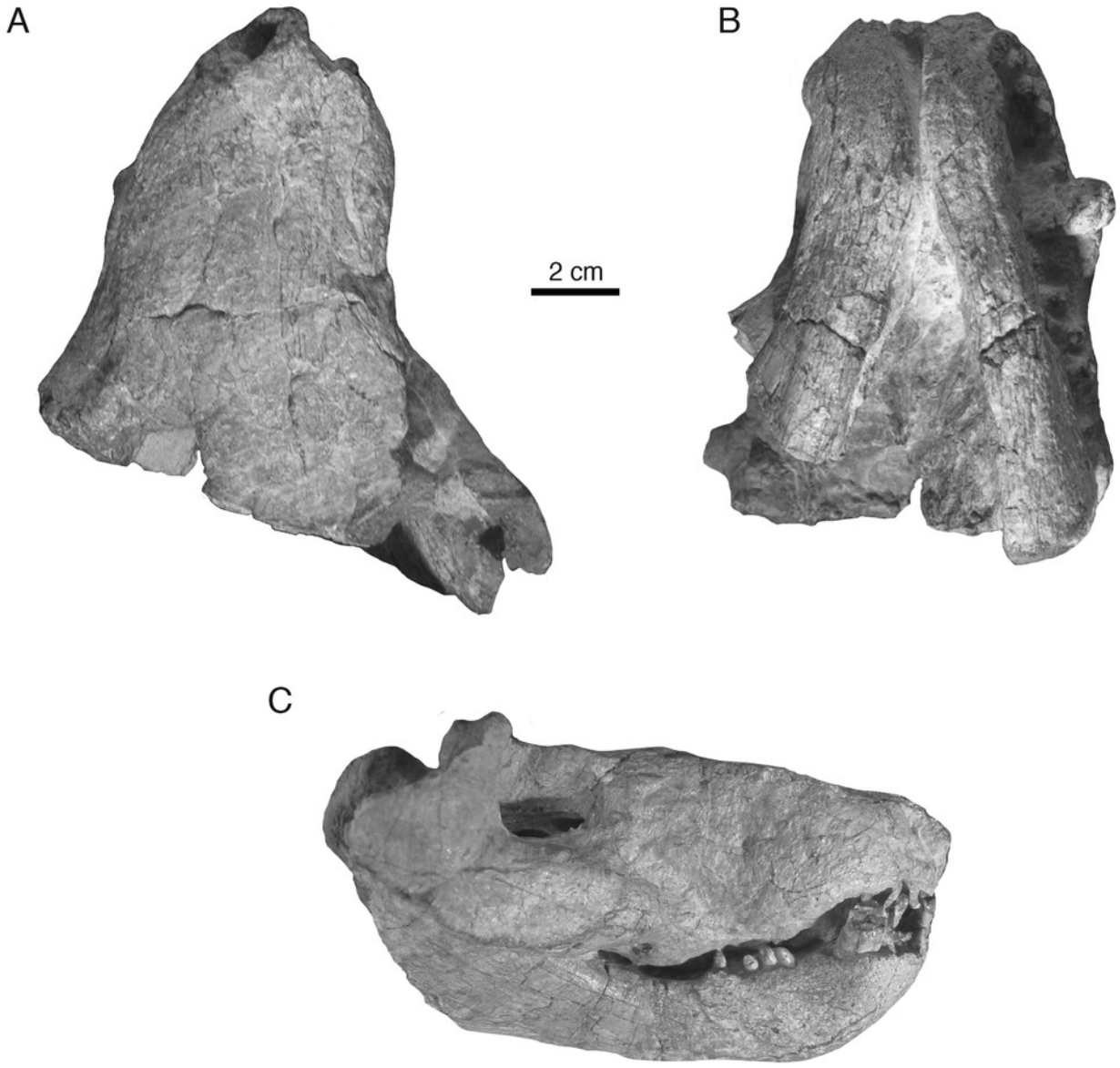

# Figure 3

Interpretive line drawings of the holotypic skull of *Microwhaitsia mendrezi* gen. et sp. nov. (SAM-PK-K10990) in dorsal (A), ventral (B), and right lateral (C) views.

**Abbreviations**: **d**, dentary; **C**, upper canine; **cr.ch**, crista choanalis; **f**, frontal; **f.l**, lacrimal foramen; **I5**, fifth upper incisor; **j**, jugal; **l**, lacrimal; **m**, maxilla; **n**, nasal; **p**, parietal; **pal**, palatine; **pC**, upper precanine; **PC5**, fifth upper postcanine; **po**, postorbital; **pm**, premaxilla; **prf**, prefrontal; **pt**, pterygoid; **sa**, surangular; **sm**, septomaxilla; **sp**, splenial.

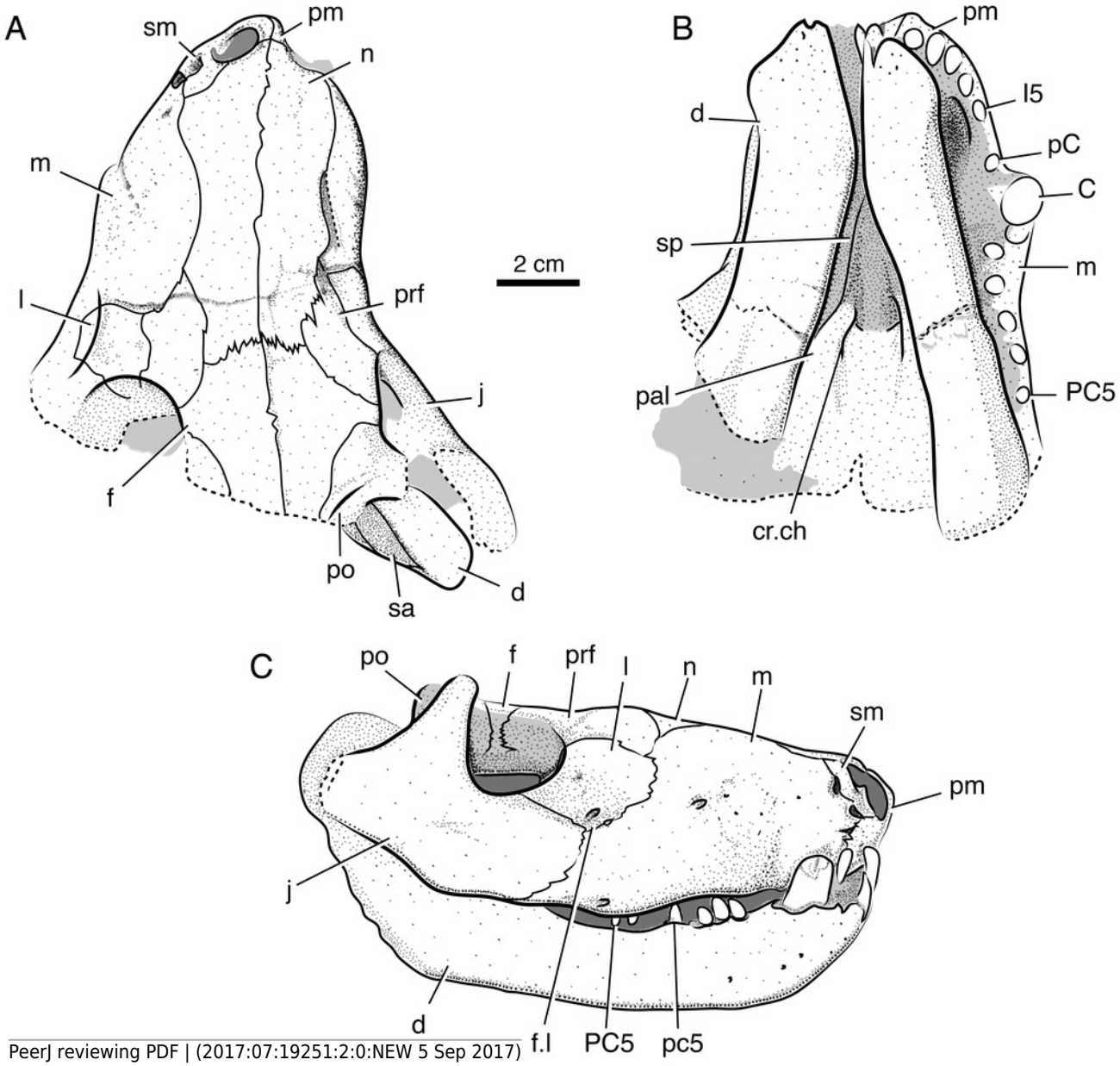

# Figure 4

Stereopair images of the palate of the holotypic skull of *Microwhaitsia mendrezi* gen. et sp. nov. (SAM-PK-K10990) in left oblique ventral (A) and posteroventral (B) views.

Note the narrow contact between the left crista choanalis and vomer without sutural connection

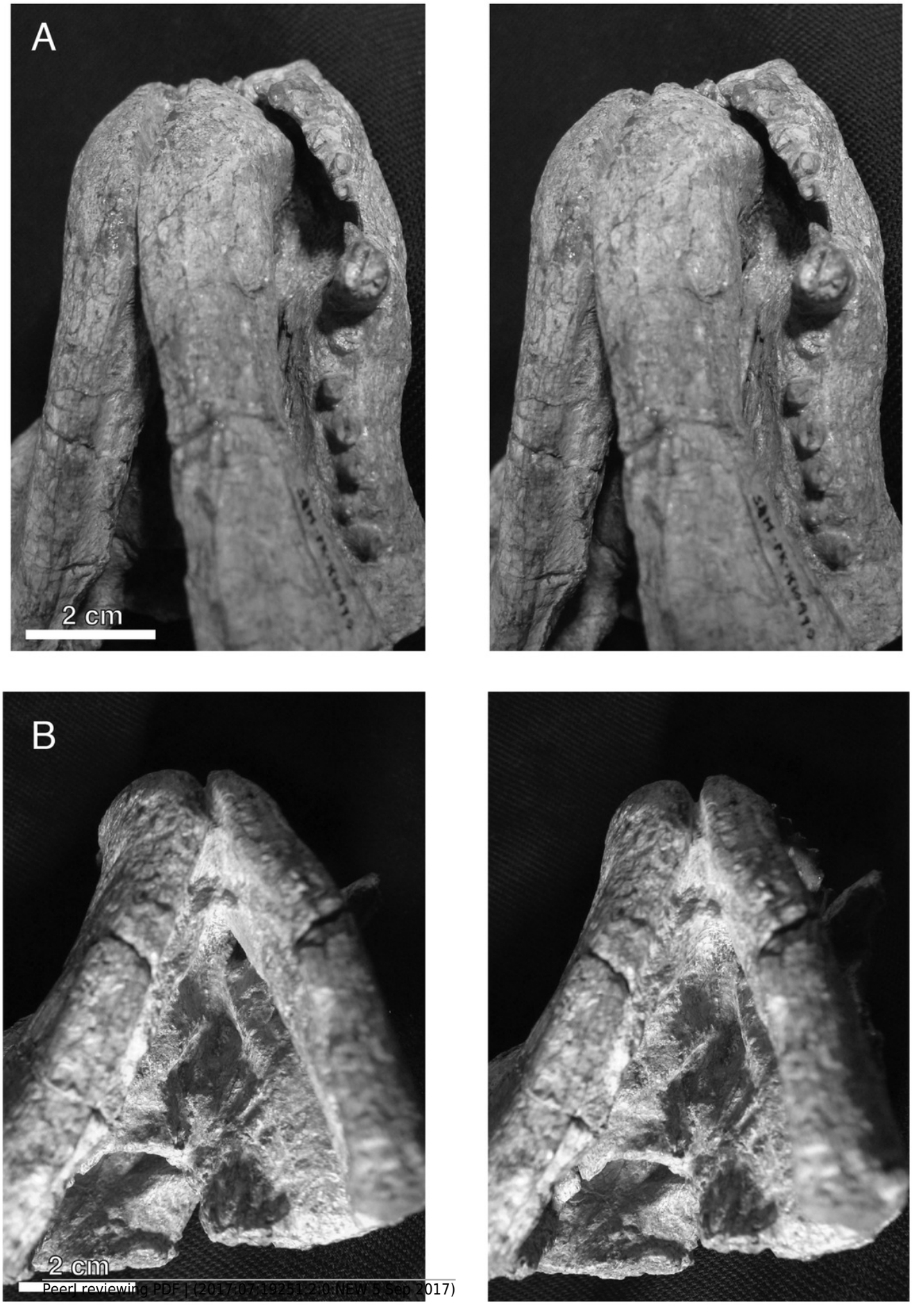
A
2 cm
B
2 cm

# Figure 5

Referred specimen of *Microwhaitsia mendrezi* gen. et sp. nov. (SAM-PK-K10984) in dorsal (A), ventral (B), and left lateral (C) views.

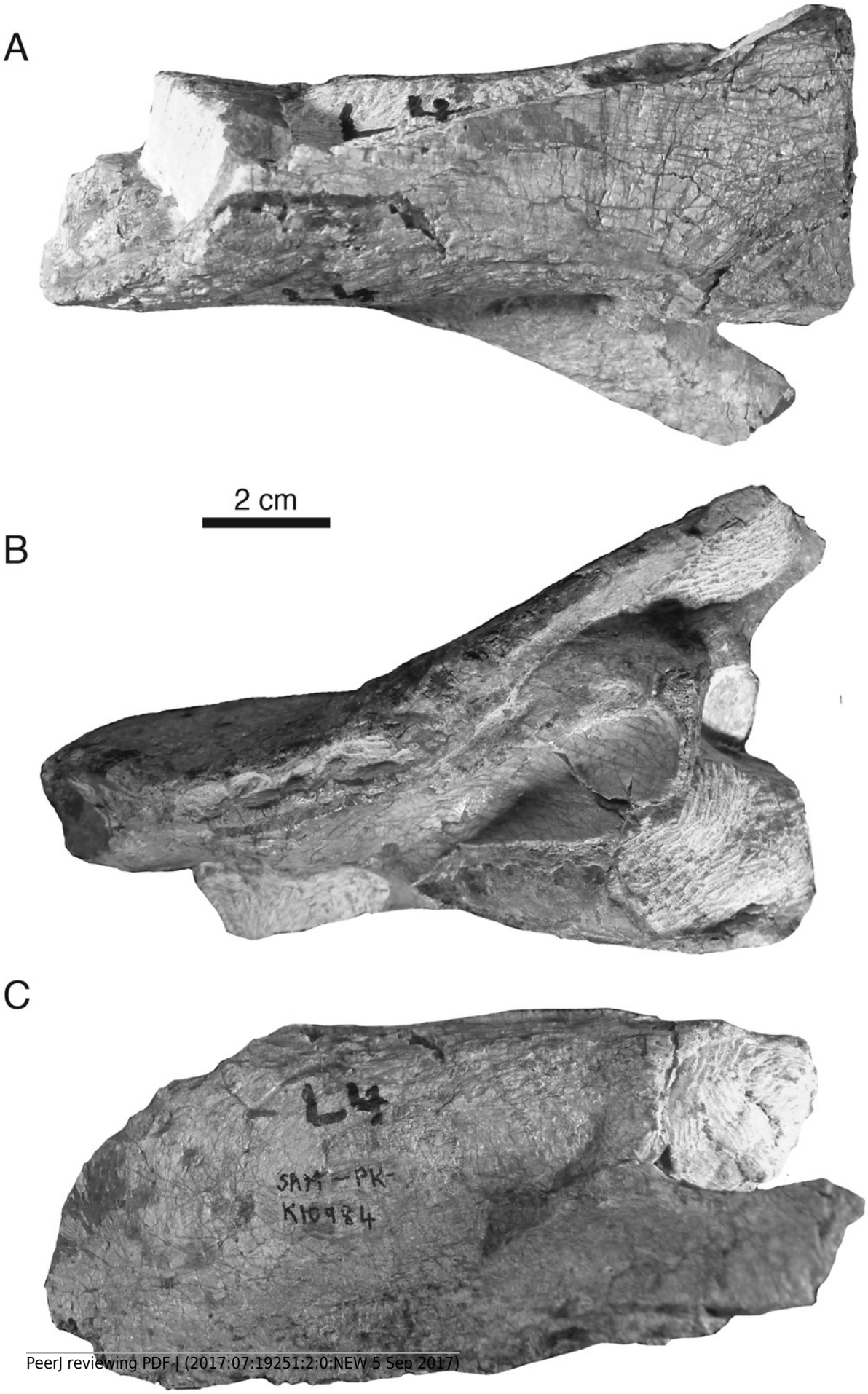
A
2 cm
B
C
L4
SAM-PK-
K10984

# Figure 6

Interpretive line drawings of referred specimen of *Microwhaitsia mendrezi* gen. et sp. nov. (SAM-PK-K10984) in dorsal (A), ventral (B), and left lateral (C) views.

**Abbreviations**: **C**, upper canine alveolus; **cr.ch**, crista choanalis; **ect**, ectopterygoid; **f**, frontal; **j**, jugal; **l**, lacrimal; **m**, maxilla; **m.pal.f**, maxillo-palatine foramen; **n**, nasal; **pal**, palatine; **PC5**, fifth upper postcanine alveolus; **prf**, prefrontal; **pt**, pterygoid; **v**, vomer; **v.suborb**, suborbital vacuity.

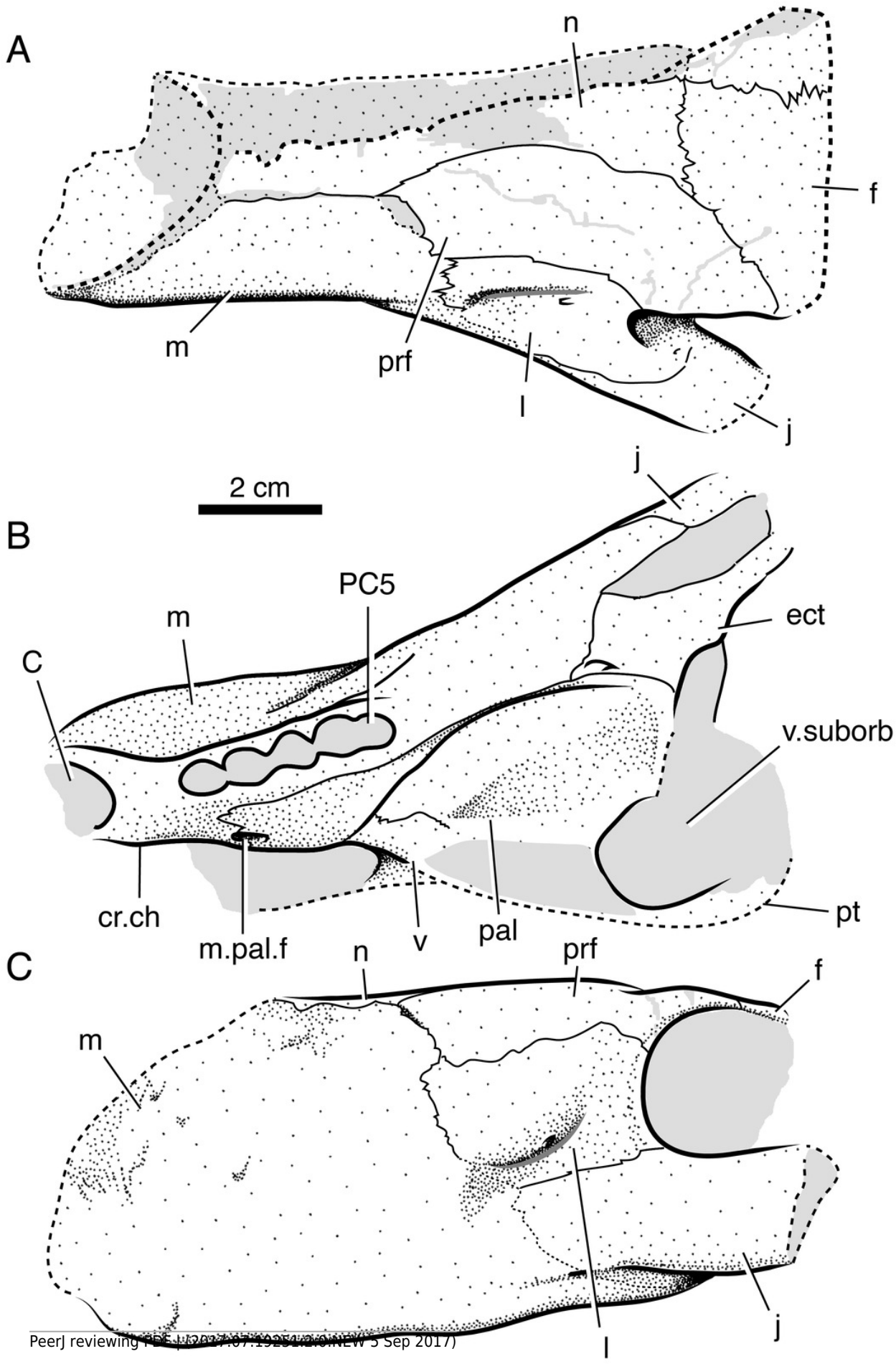
A
n
f
m
prf
l
j
2 cm
B
j
PC5
m
ect
C
v.suborb
cr.ch
m.pal.f
v
pal
pt
C
n
prf
f
m
l
j

# Figure 7

Volumized HRXCT scans of the skull of *Ophidostoma tatarinovi* gen. et sp. nov. (SAM-PK-K8516) in dorsal (A), ventral (B), left lateral (C), and frontal (D) views.

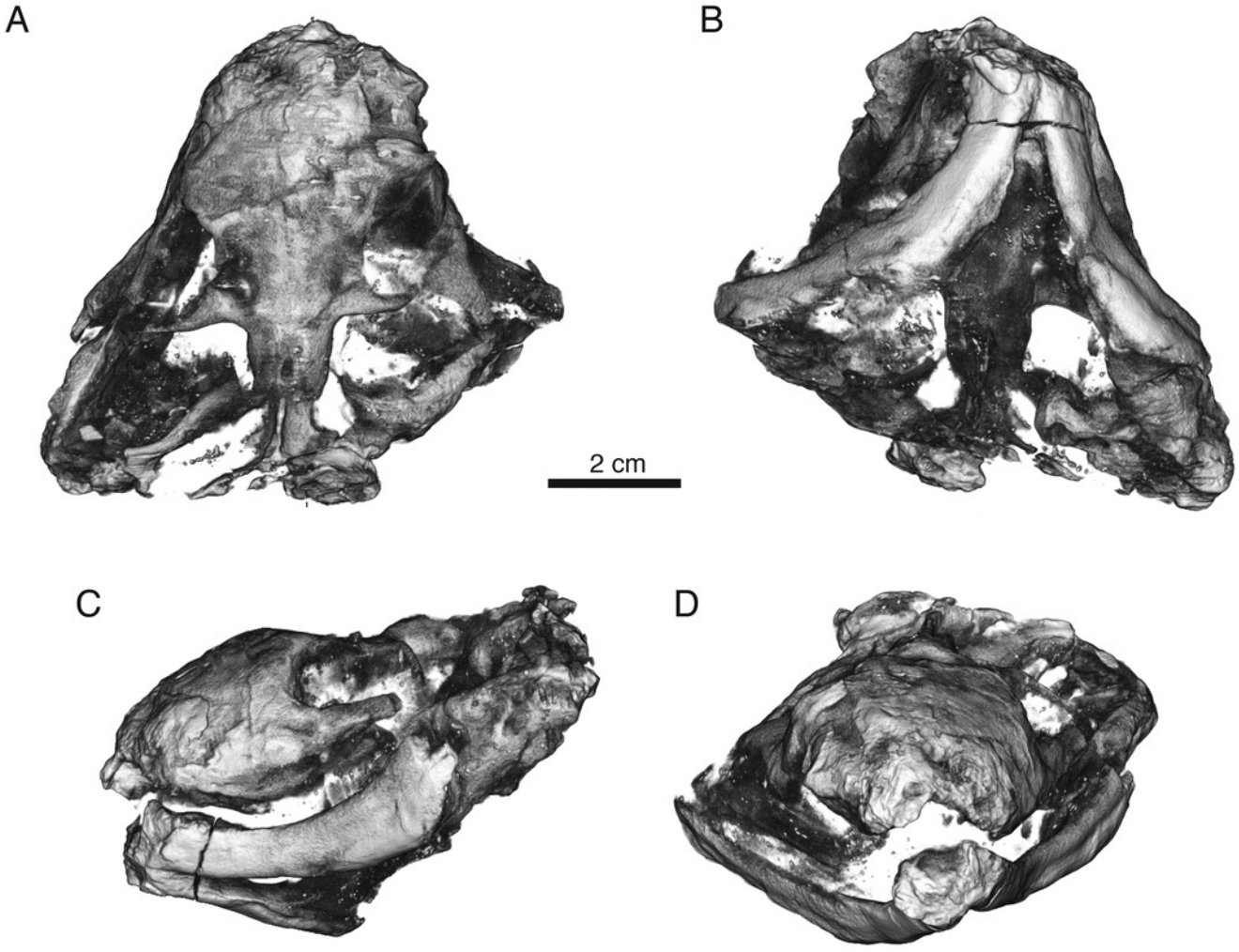

# Figure 8

Interpretive line drawings of the skull of *Ophidostoma tatarinovi* gen. et sp. nov. (SAM-PK-K8516) in dorsal (A), ventral (B), left lateral (C), and frontal (D) views.

**Abbreviations**: **a**, angular; **d**, dentary; **ect**, ectopterygoid; **c**, lower canine; **C**, upper canine; **f**, frontal; **fen.m**, mandibular fenestra; **i**, lower incisor; **j**, jugal; **l**, lacrimal; **m**, maxilla; **n**, nasal; **p**, parietal; **part**, prearticular; **pbs**, para-basisphenoid; **PC6**, sixth upper postcanine; **po**, postorbital; **pm**, premaxilla; **prf**, prefrontal; **pt**, pterygoid; **q-qj**, quadrate-quadratojugal complex; **sa**, surangular; **sm**, septomaxilla; **sp**, splenial; **sq**, squamosal; **v.ipt**, interpterygoid vacuity; **v.suborb**, suborbital vacuity.

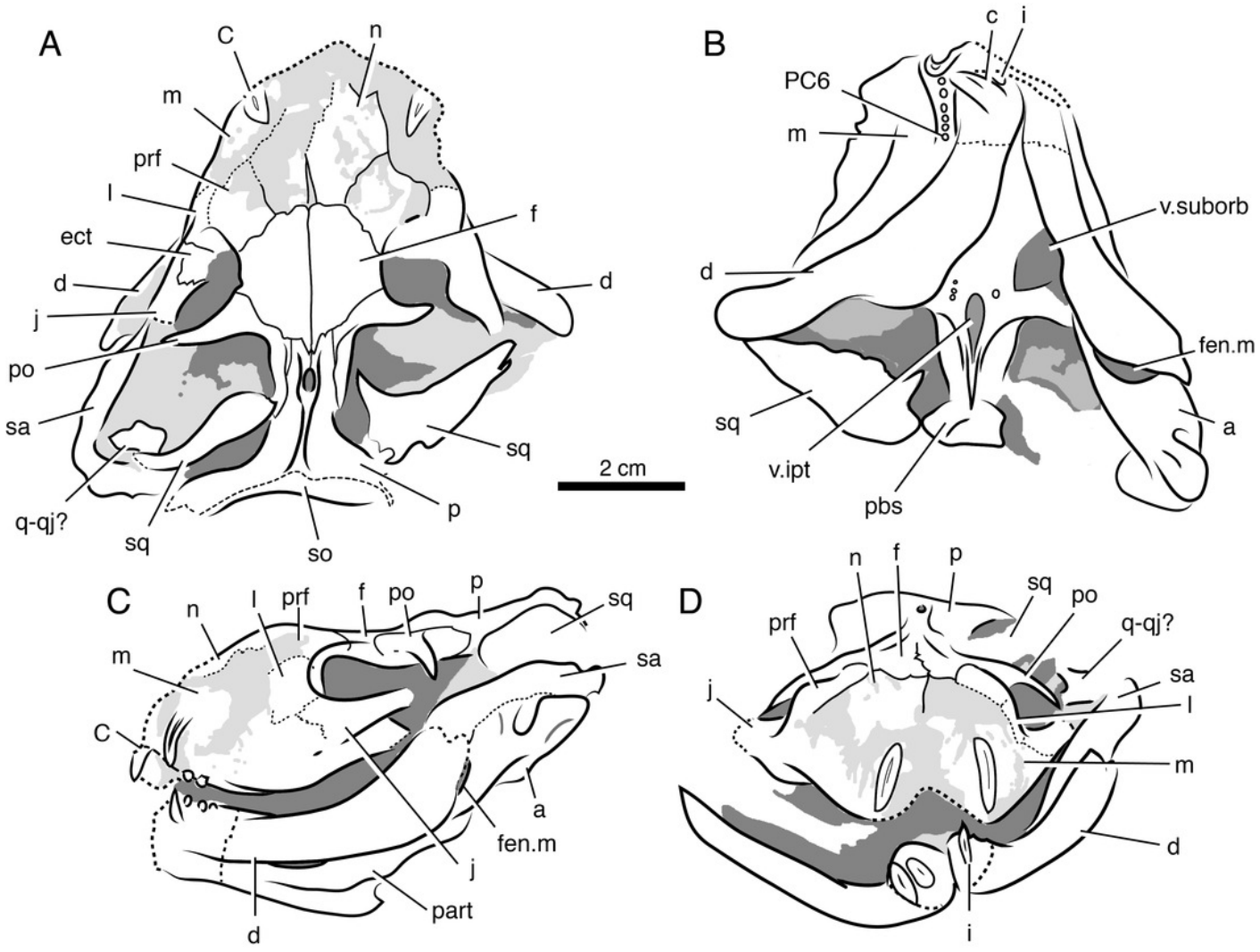

# Figure 9

Conservative phylogenetic relationships of the major clades of eutherocephalians, showing conflicting arrangements obtained from Bayesian and parsimony analyses as polytomies (tree length = 381; consistency index (CI) = 0.438; retention index = 0.789; res

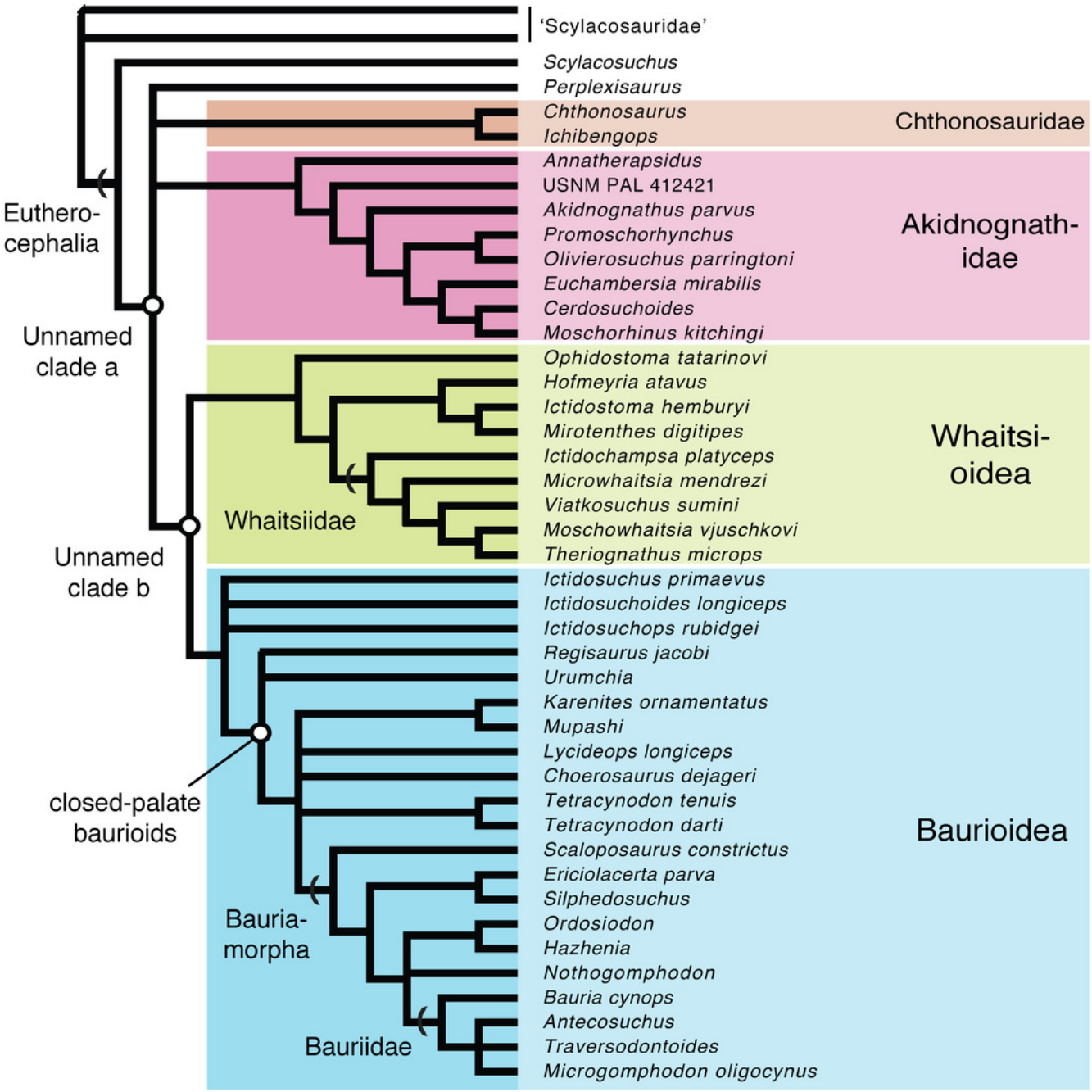

# Figure 10

New specimen of the hofmeyriid *Mirotenthes digitipes* Attridge, 1956 (SAM-PKK11188) from the upper *Cistecephalus* Assemblage Zone of 'Good Luck.'

Specimen shown in dorsal oblique view, showing the large temporal fenestra and broad, anvil-shaped epipterygoid (**ept**) processus ascendens.

# Figure 11

Stratigraphically calibrated phylogeny of middle Permian through Triassic therocephalians showing calibration points for minimum divergence dates of major clades (A).

Light gray lines represent hypothetical phylogenetic branching, whereas black bars represent observed stratigraphic ranges (dashed ends indicate taxa having unknown upper or lower ranges). Graph (B) shows peak levels of eutherocephalian origination/extinction by the Wuchiapingian stage. **Abbreviations**: **An**, Antarctica; **Ch**, China; **Chx**, Changxingian; ***Ci*AZ**, *Cistecephalus* Assemblage Zone; ***Dapto*AZ**, *Daptocephalus* Assemblage Zone; **Ind**, Induan; **Na**, Namibia; **Olen**, Olenekian; ***Prist*AZ**, *Pristerognathus* Assemblage Zone; **Roa**, Roadian; **Ru**, Russia; **SA**, South Africa; ***Tapino*AZ**, *Tapinocephalus* Assemblage Zone; ***Tr*AZ**, *Tropidostoma* Assemblage Zone; **Tz**, Tanzania; **Wor**, Wordian; **Za**, Zambia.

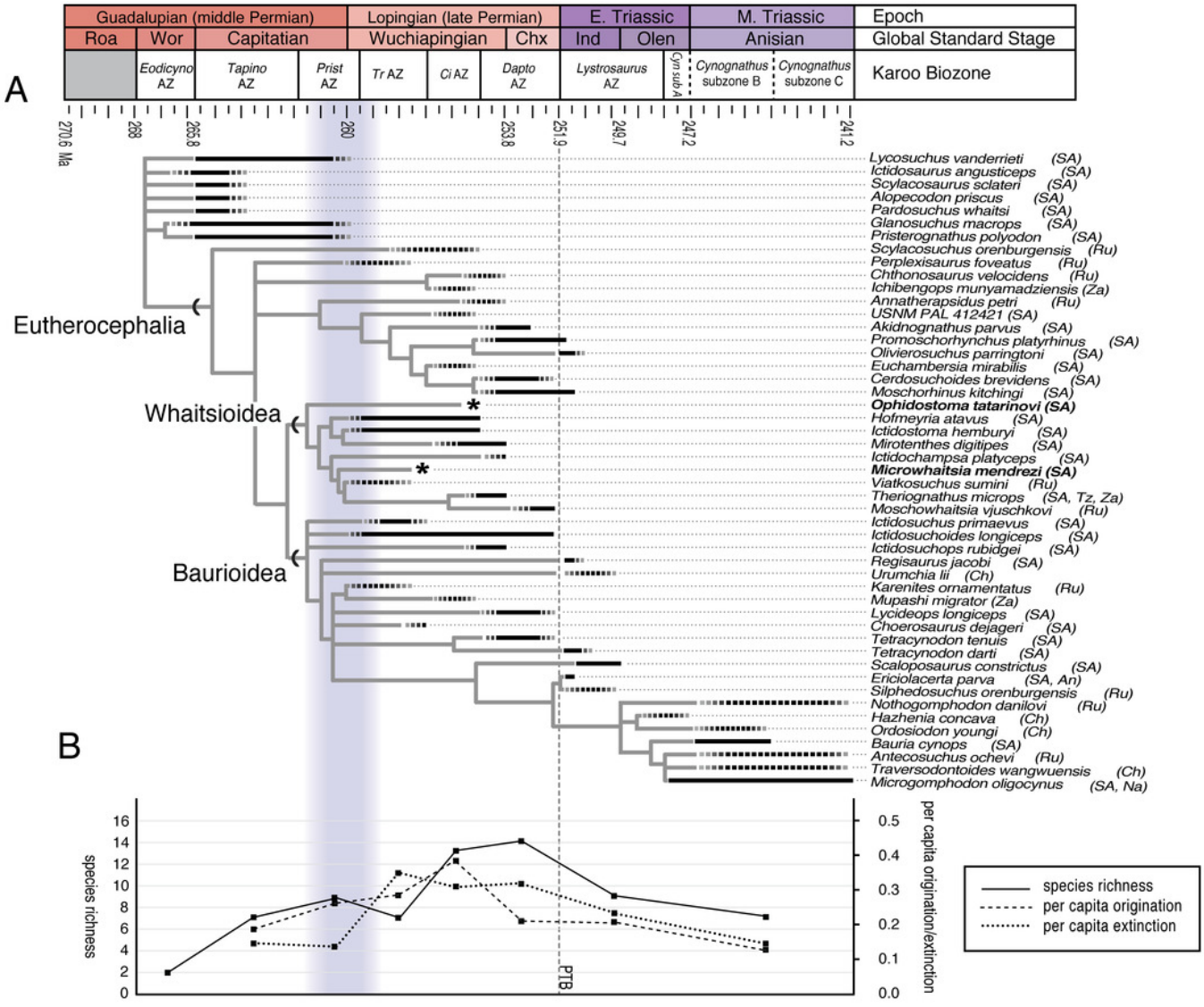
A
Guadalupian (middle Permian)
Lopingian (late Permian)
E. Triassic
M. Triassic
Epoch
Roa
Wor
Capitatian
Wuchiapingian
Chx
Ind
Olen
Anisian
Global Standard Stage
Eodicyno AZ
Tapino AZ
Prist AZ
Tr AZ
Ci AZ
Dapto AZ
Lystrosaurus AZ
Cyn sub A
Cynognathus subzone B
Cynognathus subzone C
Karoo Biozone
270.6 Ma
268
265.8
260
253.8
251.9
249.7
247.2
241.2
Eutherocephalia
Whaitsioidea
Baurioidea
Lycosuchus vanderrieti (SA)
Ictidosaurus angusticeps (SA)
Scylacosaurus sclateri (SA)
Alopecodon priscus (SA)
Pardosuchus whaitsi (SA)
Glanosuchus macrops (SA)
Pristerognathus polyodon (SA)
Scylacosuchus orenburgensis (Ru)
Perplexisaurus foveatus (Ru)
Chthonosaurus velocidens (Ru)
Ichibengops munyamadziensis (Za)
Annatherapsidus petri (Ru)
USNM PAL 412421 (SA)
Akidnognathus parvus (SA)
Promoschorhynchus platyrhinus (SA)
Olivierosuchus parringtoni (SA)
Euchambersia mirabilis (SA)
Cerdosuchoides brevidens (SA)
Moschorhinus kitchingi (SA)
Ophidostoma tatarinovi (SA)
Hofmeyria atavus (SA)
Ictidostoma hemburyi (SA)
Mirotenthes digitipes (SA)
Ictidochampsa platyceps (SA)
Microwhaitsia mendrezi (SA)
Viatkosuchus sumini (Ru)
Theriognathus microps (SA, Tz, Za)
Moschowhaitsia vjuschkovi (Ru)
Ictidosuchus primaevus (SA)
Ictidosuchoides longiceps (SA)
Ictidosuchops rubidgei (SA)
Regisaurus jacobi (SA)
Urumchia lii (Ch)
Karenites ornamentatus (Ru)
Mupashi migrator (Za)
Lycideops longiceps (SA)
Choerosaurus dejageri (SA)
Tetracynodon tenuis (SA)
Tetracynodon darti (SA)
Scaloposaurus constrictus (SA)
Ericiolacerta parva (SA, An)
Silphedosuchus orenburgensis (Ru)
Nothogomphodon danilovi (Ru)
Hazhenia concava (Ch)
Ordosiodon youngi (Ch)
Bauria cynops (SA)
Antecosuchus ochevi (Ru)
Traversodontoides wangwuensis (Ch)
Microgomphodon oligocynus (SA, Na)
B
species richness
per capita origination/extinction
PTB
species richness
per capita origination
per capita extinction

# Figure 12

Representative hofmeyriid from the late Capitanian or earliest Wuchiapingian of the Karoo Basin, South Africa, compared to other known specimens of *Hofmeyria*.

SAM-PK-K10525 (**A**), Hofmeyriidae from the *Pristerognathus* Assemblage Zone of Lombardskraal, Beaufort West district, Western Cape Province. Specimen shows short, high rostrum, prefrontal-postorbital contact in orbit, anteriorly expanded epipterygoid, and conical, non-serrated/non-carinated maxillary teeth. BP/1/4404 (BP, former Bernard Price Institute, now Evolutionary Studies Institute, Johannesburg) (**B**), *Hofmeyria* cf. *H. atavus* from the *Cistecephalus* Assemblage Zone of Matjiesfontein (Highlands), Victoria West district, Northern Cape Province. BP/1/1399 (**C**), *Hofmeyria* cf. *H. atavus* from the *Cistecephalus* Assemblage Zone of Driehoeksfontein, Murraysburg district, Western Cape Province. Numbers 14–136 are characters listed in the phylogenetic analysis (see online Supplemental Appendix) followed by the derived state in parentheses corresponding to hofmeyriids or other early whaitsioids. **Abbreviations**: **AZ**, Assemblage Zone; **PC**, postcanine position #.

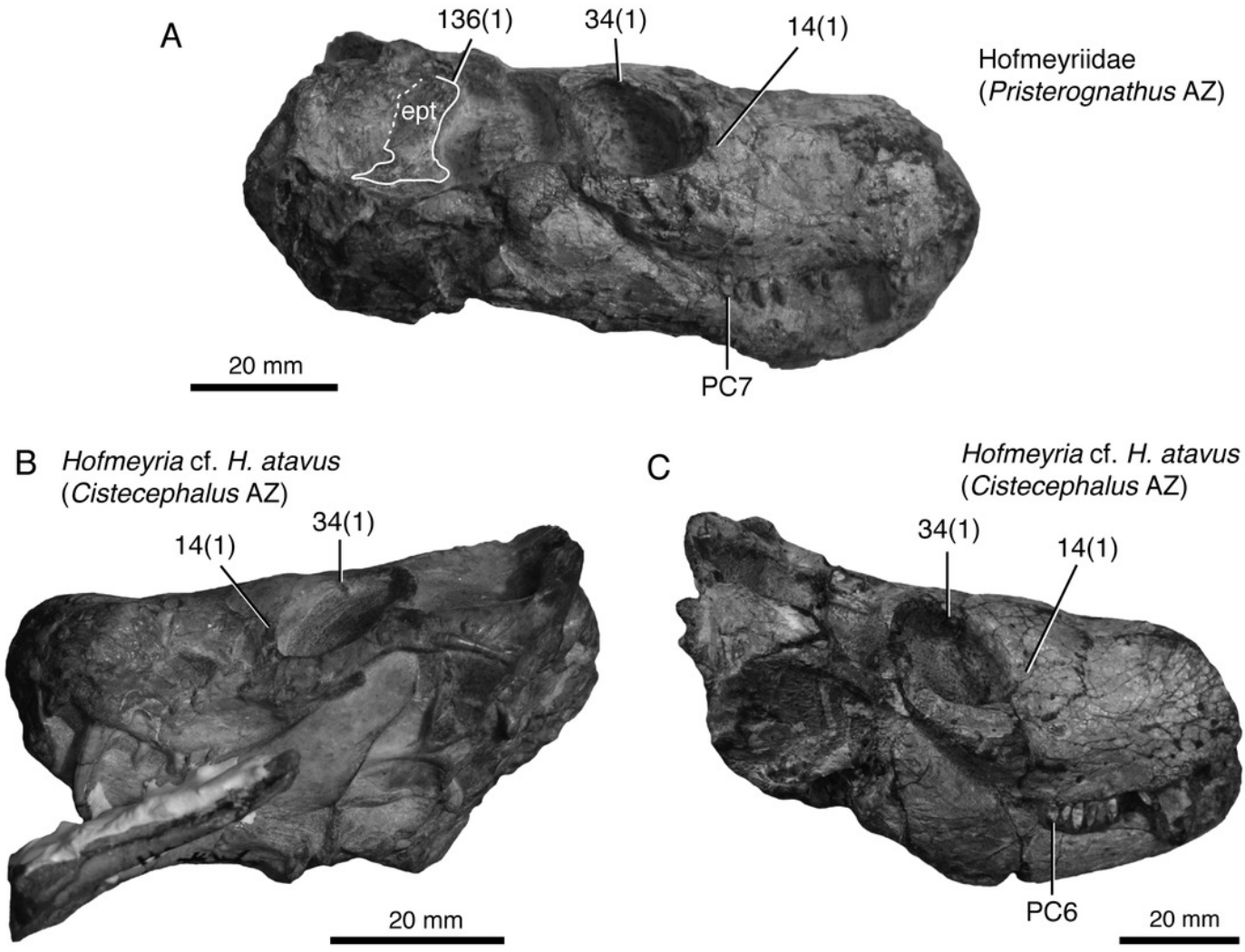
A
136(1)
34(1)
14(1)
ept
Hofmeyriidae
(*Pristerognathus* AZ)
20 mm
PC7
B
*Hofmeyria* cf. *H. atavus*
(*Cistecephalus* AZ)
14(1)
34(1)
20 mm
C
*Hofmeyria* cf. *H. atavus*
(*Cistecephalus* AZ)
34(1)
14(1)
PC6
20 mm